REVIEW ARTICLE

Microfluidics and photonics for Bio-System-on-a-Chip: A review of advancements in technology towards a microfluidic flow cytometry chip

Jessica Godin[1], *Chun-Hao Chen*[1], *Sung Hwan Cho*[1], *Wen Qiao*[2,1], *Frank Tsai*[1] *and Yu-Hwa Lo*[1]

[1] University of California, San Diego, Department of Electrical and Computer Engineering, La Jolla, CA, USA
[2] Zhejiang University, State Key Laboratory, National Engineering Research Center (NERC) for Optical Instrument, Zhejiang, Hangzhou, China

Microfluidics and photonics come together to form a field commonly referred to as 'optofluidics'. Flow cytometry provides the field with a technology base from which both microfluidic and photonic components be developed and integrated into a useful device. This article reviews some of the more recent developments to familiarize a reader with the current state of the technologies and also highlights the requirements of the device and how researchers are working to meet these needs.

A microfluidic flow cytometer protoype employing on-chip lenses for illumination and light collection in conjunction with a microfluidic sample flow system for device miniaturization.
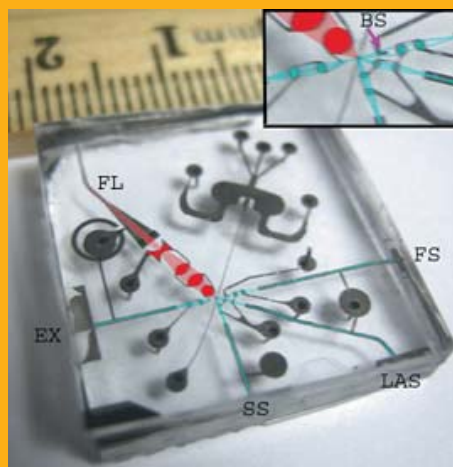
1. Introduction

Over the past decade, the field of microfluidics has begun to show great promise for research assays and diagnostics as well as for clinical applications. The field has evolved from devices comprised of simple microfluidic channels into complex devices that can mix fluids [1], pump liquids [2], perform digital logic [3–6], individually culture cells [7], determine optimal reaction conditions [8], and much more. Small-

---

*Corresponding author: e-mail: jgodin@logroup.ucsd.edu

scale fluidic devices, by definition, will have a low Reynolds number, making controlled laminar flow systems easily achievable. Microfluidics further offers the advantages of small size for miniaturization and parallelization of devices. Furthermore, this small size opens the door to the potential of portable devices. Additionally, typical fabrication processes often readily lend themselves to mass production, potentially helping to create lower-cost devices. With these advantages, the idea of low-cost lab-on-a-chip devices can start to become a reality [9]. Such devices would be very useful to researchers, clinical laboratories, and point-of-care clinicians in remote and/or resource-poor settings.

The functionality of microfluidics will expand greatly if these devices can be combined with photonics to create a new technology platform: integrated microfluidic photonics, often referred to as optofluidics [10]. Embracing photonics is a logical path of evolution for microfluidics, as the most popular techniques for biological and chemical detection are photonic in nature. Fluorescence, fluorescence resonance energy transfer (FRET), optical scattering, and surface-enhanced Raman spectroscopy (SERS) are some the most effective and accurate methods to detect analytes at the cellular and molecular level. Integration of microfluidics with photonics represents not only a new technology platform but also a transformation to the new paradigm of bio-system-on-a-chip (BSoC) [11]. As electronic integrated circuits have transformed the world of electronics, integrated microfluidic photonic circuits hold the promise to revolutionize the field of biomedicine. In spite of the rapid advances in microfluidics and photonics, however, the field is admittedly still in its embryonic stage. Technological innovations and breakthroughs are needed to demonstrate the performance and cost advantages offered through miniaturization and integration. Given the diversity of the applications, target application is needed to guide the technology development; a bio-system that is not only the workhorse for the industry but also a test vehicle to assess and benchmark the technology. The flow cytometer, or FACS (fluorescence-activated cell sorter), is just the candidate to meet these requirements.

Flow cytometers are commonly-used research and clinical tool in which the properties of each component of a sample, such as cells, are individually measured. A flow system brings cells one by one past an interrogation point, where they are illuminated by a light source. Typically the system is comprised of fluid flow through a small laser beam. As each analyte is illuminated, it scatters light with a characteristic directional intensity distribution. Further, fluorescently tagged antibodies are often used to mark and identify cells (immunofluorescence). Fluorescence may also be measured when stains are used (to quantify DNA content, show cell viability, etc), or when fluorescent proteins are present (for example when used as reporters in research settings). Thus light scattered from the cell and one or more colors of fluorescence emitted from the illuminated cell are measured, providing a number of parameters to yield statistics about the samples subpopulations. In addition, many machines have a sorting apparatus to isolate analytes of interest for further study.

The development of new cytometers is typically focused on either enhancing performance (higher throughput, more measurable parameters) or increasing accessibility (smaller, less expensive machines). The cytometer is almost inherently microfluidic in nature, rapidly interrogating small volumes of fluid. Taking the cytometer to a microfluidic platform could transform the device into a smaller, possibly mass-producible machine, and may be able to address performance enhancement as well. The cost of the cytometer, currently around $30,000 for more basic research models and more typically on the order of $100,000, could be significantly lowered, opening up new markets that were previously inaccessible due to prohibitive costs. Additionally, microfluidic cartridges could potentially be disposable, supplying a sterile device as well as containing and limiting exposure to biohazardous materials such as blood. Disposable devices also bypass the issue of device clogging, a problem experienced in benchtop cytometry, by allowing the user to quickly replace the microfluidic cartridge and continue their work. Microfluidic devices may further be able to reduce the sample size necessary for some assays, such as T-cell enumeration for HIV patients, limiting the amount of blood needed from patients as well as reducing the necessary volume of costly reagents, helping to lower testing costs.

As with any new technology platform, though, there are a number of obstacles that must be overcome to realize a practical microfluidic flow cytometer. Recent research has made great headway on a number of fronts. This article takes a look at recent progress towards the achievement of a lab-on-a-chip flow cytometer. The basic cytometer includes (i) a fluidic system, (ii) an optical interrogation system and systems for light collection, and often (iii) a cell sorting apparatus. Advances pertaining to each of these components will be discussed.

The Basics of Flow Cytometry

There are many sources that give excellent, detailed descriptions of the nature and history of flow cytometers, as well as their operation and applications [12, 13]. These references will give a comprehensive tutorial on flow cytometry; to balance completeness

and brevity, only a brief overview will be given here. To create a usable microfabricated flow cytometer, the necessity and use of each of the basic components of the benchtop device must be understood and considered.

The device contains a fluidic system for pumping both sheath flow and sample flow through the flow chamber. The interrogation source is typically a laser, 488 nm being the standard for flow cytometry. Many commercial instruments include multiple light sources, especially more high-end devices. Many newer instruments now employ lower-powered, smaller solid state lasers. Low-cost devices already tend to use alternative wavelength (such as 532 nm) diode lasers as their main sources, and violet laser diodes (VLDs) have recently received a great deal of attention as the next possible low-cost biomedical laser source [14].

The basic concept of flow cytometry is to use light signals to identify a cell in flow. For the machine to work, light must be collected from a single cell at a time with enough fidelity to ensure accurate interpretation. This means that the interrogation conditions of each cell must be identical to that of the last (light intensity, beam width, cell location in detection area). Light must be collected from a highly localized area to prevent cross-talk, and collected background light must be low enough to allow the resolution of a clear signal.

Both scattered light and fluorescence are generally collected by a flow cytometer. Two light scattering collection lines, for forward scatter collection (FSC) and side scatter collection (SSC), are typically used. Forward scatter generally requires the use of a beam stop to prevent direct receipt of the illumination source. As a particle passes through the illumination beam, an increase in light intensity will be recorded from the forward scatter line. The relative intensity is indicative of the particles identity, due to factors such as its size and refractive index. If the beam block is absent, the light collected is 'extinction'; that is, the detector will measure a dip in light intensity due to scattering from and absorption by the particle. This measurement is unusual in commercial devices. The side (or 'orthogonal') scatter line is traditionally centered perpendicular to the axis of illumination. The relative light intensity recorded on the SSC line as a particle passes is also indicative of the particles identity, generally related to the internal granularity of the particle. In addition to light scatter, several bands of fluorescence (FL) from the particle are often collected. A simple machine might include only 3 fluorescence channels, whereas more high-end instruments might have 10 or more. Each light collection line terminates in a photodetector, generally a photomultiplier tube (PMT). Forward scatter lines often employ a simple photodiode, due to their lower cost and the rela-

tively high light intensity seen on the FSC line. The fluorescence line will further require dichroic mirrors, to split the beam off to several detectors based on wavelength bands, and optical filters, to define the band of light passed to each fluorescence detector. The measured signal intensities for each parameter are used to distinguish between various sample subpopulations (e.g. monocytes, lymphocytes, and granulocytes in a leukocyte sample).

After optical detection and cell analysis, the sorting of targeted cells is performed downstream of the cytometer. As cells approach the sorting chamber, vibrations break the stream up into charged droplets, which in turn carry the cells down to a pair of electrically charged deflecting plates. Through a feedback control system (e.g. the decision making process after the cell is detected and identified upstream), the polarity of the plates changes to deflect cells of interest into the collection tube. Typically the sorting rate is on the order of 10,000–100,000 cells/s and is limited by the speed individual droplets that can be formed.

The Microfluidic Cytometer

At its simplest, microfluidic flow cytometry chip consists of a simple microfluidic channel for sample flow. Detection is accomplished by focusing a laser into the channel and coupling out light (generally via microscope objective) to a PMT, CCD, or APD [schematic]. Fluidic control is accomplished via gravity fed systems, syringe pumps, or similar mechanisms. Some of the earliest microfluidic cytometry devices were created using techniques that had been streamlined by electronics microfabrication techniques. Channels would be etched into silicon substrates [15, 16] and sealed by the bonding of lid, such as glass. These devices offered the benefits of mass-producibility and low sample volume usage (thus low reagent volume usage). Glass-etched devices offered increased flexibility in laser and detector placement and also lowered sidewall reflections due to the use of an optically transparent substrate.

With the advent and popularization of soft lithography techniques [17] (and the associated polymer replica molding techniques), the field of microfluidics has begun to take off. In this process, photolithography techniques are used to create a 'mold' from which polymer 'replicas' can be generated. Devices could now be rapidly and inexpensively prototyped, as design changes simply require the printing of new high-resolution transparency mask. Thus, polydimethylsiloxane (PDMS) based devices have become the vehicle of choice for many researchers, including those in the area of microfluidic flow cytometry.

In addition to rapid, inexpensive prototyping, PDMS also offers simple processing techniques.

After the initial mold fabrication and coating with a hydrophobic release agent, the processing does not require harmful acid-based chemistry that is common in other fabrication methods, such as direct etching of channels into glass or silicon. PDMS is an optically transparent elastomer, a good choice for the molding process and also for creating devices that will be optically interrogated. There are a number of methods for bonding PDMS to glass, polymers such as PDMS, and other materials; these methods include including partial-cure bonding [18], oxygen plasma or UV/Ozone treatment [19], corona activation [20], etc. Polymer-based microfluidic cytometers became more and more common. With the emphasis off of channel fabrication techniques, more recent research has focused on some different problems, including optical system improvement and on-chip cell sorting.

I. The Fluidic System

In a conventional flow cytometer, the potential for two or more particles to simultaneously enter the optical interrogation region is minimized by the use of flow focusing, or confining the sample flow to a very narrow stream by using the pressure of a surrounding sheath flow stream. Flow focusing further ensures uniform particle velocity by removing the sample flow from contact with the flow cell walls, reducing the parabolic flow profile that would otherwise exist. Variations in particle velocities would not only undermine the reliability of the detected signals, they can also cause synchronization problems downstream for cell sorting. Flow focusing ensures the quality, reliability, and reproducibility of the collected signals, and thus the incorporation of effective focusing modules into a microfluidic flow cytometer is critical. For these reasons, significant efforts have been made toward developing focusing methods that allow both two-dimensional (2D) and three-dimensional (3D) confinement.

A. Two-Dimensional Flow Focusing

Two-dimensional (2D) hydrodynamic flow focusing has been the most widely used techniques for particle confinements and has been applied to a number of applications, including multiple-outlet flow-switching [21], enumeration of beads [22] and cells [23], and deformation of DNA [24]. By adjusting the relative pressures of the sample inlet and the two sheath-flow channels, which lie perpendicular to the sample channel, Knight et al. have focused the sample flow stream down to $\sim$50 nm inside of a 10 μm

channel [25]. They have also developed a mathematical model to relate the focused width to flow resistances of the inlet, side, and outlet channels [25]. On the other hand, Lee et al. have extensively studied the effects of the relative flow rates as well as the channel aspect ratios on the width of the focused stream, both numerically and experimentally, for both circular [26] and rectangular [27] channel configurations. They have shown that the focused beam can be reduced down to the same order of magnitude of micron-sized particles for a circular channel diameter of 2.4 mm. Hydrodynamic focusing can also be achieved by applying suction at the device outlet [28, 29], which can allow fluid focusing with only a single syringe pump [29]. In addition, rather than using sheath liquids, air can be used as the sheath fluid to confine sample flow [28]. Under the same outlet suction pressure ($\sim$45 mm Hg), as the sample flow rate decreases down to a critical level ($\sim$5 ml/hr), flow stream becomes unstable and begins to break into individual droplets downstream. This feature may be attractive for microfluidic flow cytometers, as the formation of cell-containing droplets can facilitate in screening and sorting of *single* particles or cells. Moreover, the method can eliminate the need for large sheath reservoirs, lowering the cost of operation and also eliminating the need for a clean fluid source for on-site operation in non-urban settings.

In addition to using pump-induced force to constrain flow, focusing can also be achieved with electrokinetically-driven flow. Electrodes are inserted into fluidic channels and as DC bias is applied across the electrodes, electroosmotic flow is generated [30]. As sample flow enters the focusing region, where the three streams meet, the electroosmotically-induced flow will confine the sample stream (Figure 1), with the width of the focused sample stream depending on the relative electric field strength between the sample channel and the side channels. Schrum et al. have confined a sample stream containing 0.97 μm and 1.94 μm latex particles into an 8 μm stream inside of a 50 μm channel using a field strength ratio of $\sim$0.15 (100 V/cm and 700 V/cm at the sample channel and side channels, respectively) at a throughput of 34 particles/s [30]. Researchers have applied this electrokinetic focusing technique to a variety of applications including detection and sorting of DNA molecules [31], controlled sample plug injections of various sizes [32], and flow-switching [33]. Although adjusting the electrokinetically-focused beam size is relatively straightforward, instantaneous, and accurate, the required use of high voltage (on the order of kV) renders this technique impractical in most flow cytometric applications, since these high electric field can cause irreversible damage in the integrity of most biological agents (e.g. cells, proteins, etc.).
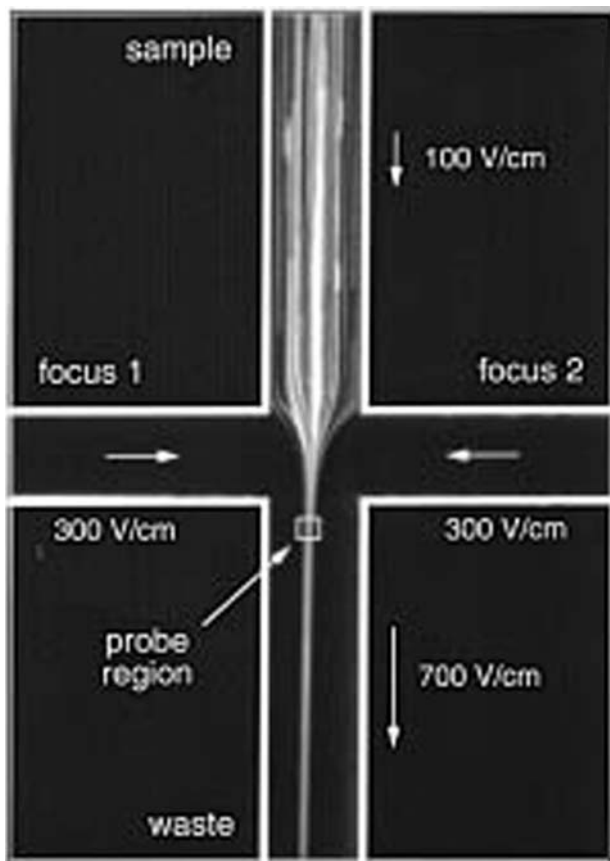
Figure 1 Time-integrated image (5 sec exposure time) showing the effects of electrokinetic focusing as electric field strengths of 100 and 300 V/cm are applied to sample and focusing (side) channels, respectively. The arrows represent both the direction of fluid movement and the relative fluid velocities in each channel. Reprinted with permission from [30]. Copyright 1999 American Chemical Society.

B. Three-Dimensional Flow Focusing

Although the conventional 2D hydrodynamic focusing involves two outer sheath flows on each side of a central sample flow to laterally constrain the sample flow, it is problematic due to the lack of vertical focusing. In the vertical direction, fluid drag along the walls creates a parabolic flow distribution, the result of which is a wide distribution of sample flow velocities. This can be problematic in terms of cross-talk; a slow cell may be 'caught up' to by a faster cell, resulting in more doublets (two cells being interrogated simultaneously). Additionally, the velocity distribution can result in variations in the detected signal from an otherwise homogenous population due to different integration times at the detector or differing illumination intensities from a nonuniform illumination beam. Lastly, for high-

speed, high accuracy cell sorting, an exact knowledge of the cells location is critical. All these factors contribute to a strong interest in developing three-dimensional (3D) focusing devices capable of confining small quantities of cells/particles in both horizontal and vertical directions. Generally speaking, there are two kinds of approaches reported for achieving 3D focusing of cells/particles in microfluidic channels: dielectrophoresis (DEP) and 3D hydrodynamic focusing.

Dielectrophoresis (DEP) is a phenomenon in which a force is exerted on a dielectric particle when it is subjected to a non-uniform electric field. Morgan et. al. demonstrated that DEP can be used to focus nanoscale latex particles as small as 40 nm in diameter [34]. Lin et al designed a flow cytometer with 3D focusing capability which was able to focus the sample stream to a width of 8 μm [35]. This feature was realized by a combination of 2D hydrodynamic forces as horizontal focusing and negative DEP forces as vertical focusing. But DEP has several intrinsic drawbacks: 1) device making requires complex fabrication process such as e-beam evaporation and precise electrode-to-substrate alignment, 2) Electric field generation entails extra electronics, and 3) liquids with specific conductivities are needed for different particles, since The DEP force heavily depends both on the nature of the particles being focused as well as on the nature of the fluid suspension.

Unlike dielectrophoresis, 3D hydrodynamic focusing acts on the fluid rather than on the particles.
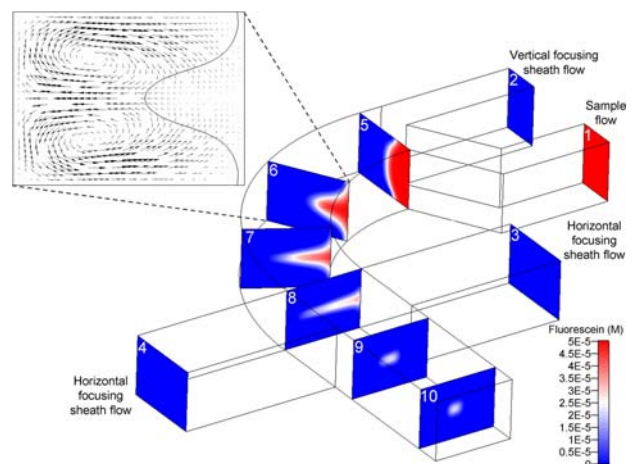
Figure 2 (online color at: www.biophotonics-journal.org) Schematic of the 3D hydrodynamic focusing process by employing the "microfluidic drifting" technique. Slices 1–10 are the cross-sectional profiles of the fluorescein dye concentration in the focusing device. Inset: the simulation of the secondary flow velocity field shows the formation of Dean Vortices in the 90-degreee curve. An iso-curve of fluorescein concentration = 25 μM is arbitrarily chosen as the boundary of the sample flow [42]. *Reproduced by permission of The Royal Society of Chemistry.*

It is achieved by completely surrounding the sample flow by sheath flow that constrains the sample flow to the center of the channel in both the lateral and the vertical dimensions. Klank et al simulated and fabricated a "chimney" structure in silicon by reactive ion etching [36, 37]. The coaxial sample sheathing was obtained by injecting a sample into the sheath flow in a perpendicular direction. However, the disadvantage is that the fabrication process is very complicated. Three-dimensional focusing has also been achieved using clever, multi-layered 3D microfluidic devices [38–41]. Most recently, Mao et al demonstrated a "microfluidic drifting" technique that enabled 3D hydrodynamic focusing with a simple single-layer planar microfluidic device fabricated via standard soft lithography [42]. Sample flow with a total height of less than 15 μm was obtained by the transverse secondary flow induced by the centrifugal effect in a curved microfluidic channel (Figure 2). This chip, which does not require assembly of individual components or multiple alignments and exposures during mold fabrication, is easy to fabricate and mass producible.

II. The Optical System

Initially, microfluidic chips were looked at as a replacement for the flow cuvette of the cytometer; all of the optical systems remained essentially the same, and often this is still the case [15, 36, 40]. For portable systems, the size and weight of the light collection system is an important consideration. Utilizing a bulk optical system drastically reduces the benefits of miniaturizing the fluidic platform by overshadowing the gains of miniaturization. Ideally, the optical system would scale down in size with the fluidic system while maintaining both the low system cost and the possibility for mass production. Additionally, reducing the size of the optical system would reduce the total optical path length, which may reduce absorption losses, an important consideration in fluorescence measurements. To address these issues, some researchers considered collecting light in close proximity to the channel by using lower-cost, small photodetectors such as avalanche photodiodes [19, 43] placed above or below the chip, making a more compact device. This approach wont work for multi-parameter detection, however, limiting its utility for flow cytometers.

A more recent approach by Kostner et al, among others, has been the use of CD or DVD pickup heads as small, low-cost, and low-powered optical interrogation and collection systems [44]. The authors were able to detect and differentiate between polystyrene beads and erythrocytes. Cells and beads are of course very different in optical properties; how-ever, future improvements and investigations could greatly improve upon this promising approach. Additionally, the work would likely need to be expanded to encompass multi-parameter detection (i.e. fluorescence) to create a more practical device.

A. Optical Fibers

By the 1980s, the cytometry community had started to make use of optical fibers in their machines and had even begun to consider the possibility of replacing conventional bulk optics with optical fibers [12]. Many in the microfluidic flow cytometry research community also began to investigate the use of alternative optics. Pamme et al. used fibers held at fixed angles above the fluidic channel to collect light scatter at 15° and 45° while using a lamp for sample illumination. Light scattering CVs were typically 25–30%; quite an achievement for a microfluidic device but considerably larger than the expected 5% variation that might be expected from a benchtop device [22]. The authors attributed this large signal distribution to effects such as scattering from sidewall roughness, illumination beam imperfections, and cross-talk. Chabinyc et al. also employed fibers, integrating them on the chip by first clamping them to the mold in close proximity to the microfluidic channel and then pouring PDMS to make the mold replica around them [19]. The glass-PDMS adhesion during polymer curing yielded a robustly-integrated optical fiber that required no index matching fluid. The method still requires some alignment and assembly, a problem which is often avoided by the use of fiber sleeves. In this approach, the mold includes a channel into which the fiber is inserted after polymer curing and epoxy-fixed in place [45]. The fiber sleeve approach can also avoid the use of index matching liquids by filling the airspace instead with a curable liquid, often the very same heat-curable polymer used to make the device itself [46].

B. Integrated Waveguides

Waveguides offer similar light-confinement capabilities to optical fibers but in a more robustly integrated fashion. Such chips would directly interface with light sources and detectors, making for a simple testbed that readily allows for chip changes. On-chip waveguides can be used to direct light to targets, such as detectors within microns of the illuminated samples without the difficulties of alignment, epoxy-fixing, or breakage. On chip waveguides fabricated by oxide deposition [47] or ion exchange [48] have been applied to on-chip detection systems. Anisotropic silicon etch-

ing has been also utilized to form metalized silicon waveguide grooves capped by metal strips. In this application, optical coupling between the waveguides and microchannels is achieved by reflection from the end-facets of the waveguides [49]. Many these methods, however, require complex and lengthy fabrication process, and often the materials are not well-suited for biological applications or for visible light.

S. H. Huang et. al. fabricated a monolithic, two-layered TIR (Total Internal Reflection)-based microfluidic chip using SU-8 photoresist to create planar waveguides [50]. An SU-8 microprism directed incoming light into the slab waveguide. The analytes were located above the waveguide. This monolithic integration allows for a higher coupling efficiency from the fiber into the waveguide (without the need for index-matching oils) and low reflectance loss on the interfaces. This polymer-based waveguide has some advantages over the non-polymer based techniques mentioned above such as low-cost fabrication, relatively simple processing, and ease of alignment, which is important for light coupling efficiency.

Monolithic waveguide integration of polymer waveguides made by PDMS with microfluidic channels is an attractive approach due to simple channel sealing, device robustness, good material optical properties, and precise alignment of waveguides and microchannels [51]. V. Lien demonstrated monolithic integration of microfluidic channels and waveguides in PDMS-based devices [52]. A higher refractive index PDMS ($n = 1.42$) was injected into core channels surrounded by cladding layers of lower refractive index PDMS ($n = 1.407$). This cost-effective method demonstrates simple prealignment and enables optical coupling between the channels and waveguides. Figure 3(a) and (b) show, respectively a prealigned waveguide structure and a side view of a device waveguide emitting fluorescent light [51]. Since the waveguides and the microchannels are self-aligned by photolithography during the mold fabrication, no fine alignment using microscope translation stages or mico-positioners is needed during fabrication.

Bliss et. al. similarly demonstrated a *liquid* optical waveguide by injecting high refractive index liquid PDMS prepolymer into the prealigned microfluidic channels [46]. By introducing uncured PDMS into the microfluidic channels as the core material of the waveguide, this method allows for cleaning and reusing of the waveguide channel. As is often done for testing waveguide-based devices, optical coupling between the liquid PDMS waveguides and light source or detectors was achieved through optical fibers inserted into the liquid-core waveguides at the edge of the microfluidics chips. The liquid PDMS pre-polymer coats the inserted fiber, reducing reflections and scattering at the optical interface, thus increasing the light coupling efficiency. The method of index matching works for cured waveguides as well. Figure 4(a) shows observed scattered light at the interface of the inserted optical fiber and uncured PDMS prepolymer waveguide. The measured loss was 2.9 dB cm^{-1} and 2.2 dB cm^{-1} at 523 nm and 633 nm, respectively. Figure 4(b) shows a plot of normalized waveguide attenuation for two different wavelengths. The light propagation loss seems to be mainly due to surface scattering by the sidewall roughness of the mold. Waveguide attenuation could be dramatically reduced if surface roughness is decreased by improvements in the mold fabrication process.

Whitesides' group has been working on liquid-core/liquid-cladding (L^2) optical waveguide which consists of a liquid core fluid with high refractive index and liquid cladding fluid with lower refractive index [53]. They used deionized water ($n_d = 1.335$) as the cladding fluid and $CaCl_2$ (aqueous, $n_d = 1.445$) as the core fluid inside the PDMS-based microfluidic channel. A stream of core fluid is released into the center of the stream of cladding fluid, and light is guided within the higher-index core fluid [10]. It was reported that at low Reynolds number ($5 \sim 500$), the liquid/liquid interfaces are optically smooth and the optical loss at the interface due to scattering was less than 1dB/cm. The authors pointed out that if the channel roughness is less than 5% of the channel width, the effect of the roughness is negligible on the optical smoothness of the interfaces. By using different fluids, the numerical aperture of the waveguide can be modified by changing the refractive index contrast ($\Delta n = n_{core} - n_{cladding}$). This

Figure 3 (online color at: www.biophotonics-journal.org) (a) Pre-aligned monolithic waveguide perpendicular to the microfluidics channel, (b) emanating fluorescent light guided by PDMS waveguide of (a) (side view). The method was later modified to use completely separate waveguide and fluidic channels [51]. © 2004 IEEE.
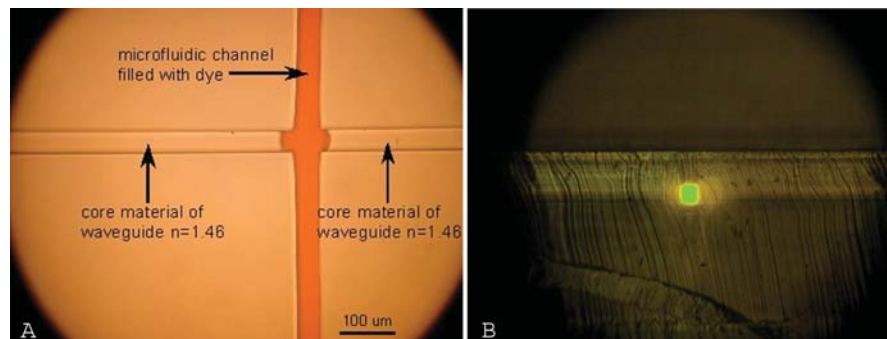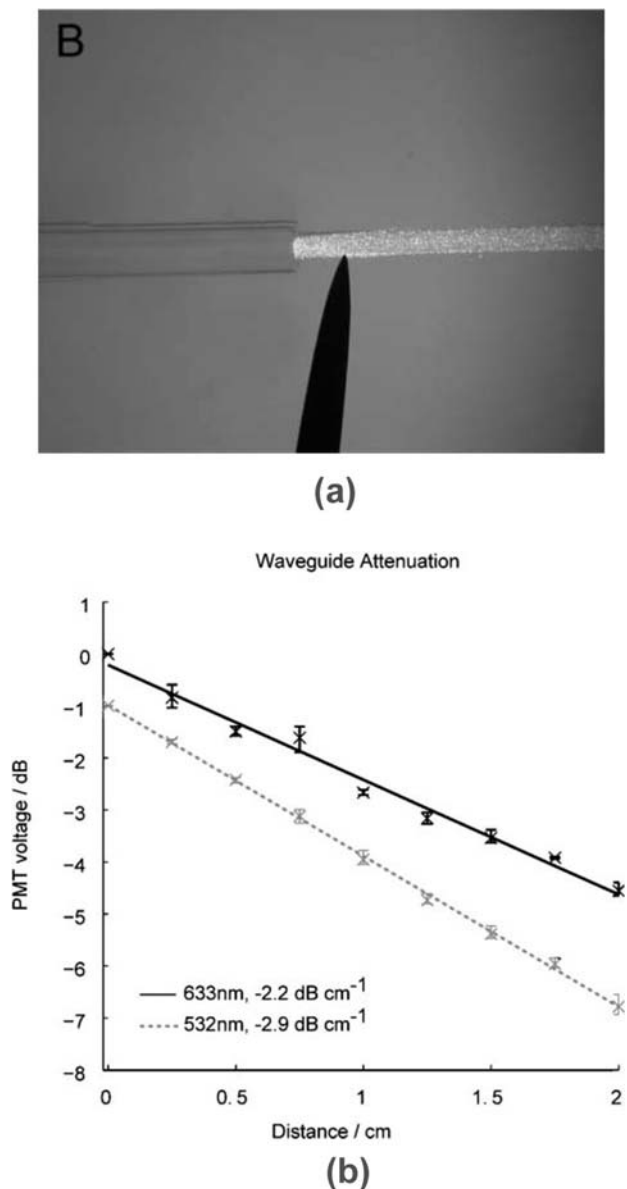
Figure 4 (a) Scattered light observed when a live fiber is inserted into the coupler (b) Plots of the normalized intensity along the PDMS waveguide demonstrating the propagation loss at 532 nm and 633 nm [46]. *Reproduced by permission of The Royal Society of Chemistry.*

method has been further expanded to include thermally generated optical waveguides [54]. In this application, the same liquid is introduced into the core and cladding channels at different temperatures. The lower temperature core liquid has a higher refractive index than the warmer cladding liquid, resulting in light guiding. The use of a single liquid would make fluid recycling easier for long-term operation; however, due to rapid thermal diffusion, it is very hard to maintain refractive index difference required for optical guiding.

These different schemes of moving the optical systems onto the microfluidic chip have several advantages, particularly for the light collection system. Close-proximity detection can theoretically allow for lower loss and higher-NA light collection due to the effectively 'immersed' optical system (no on-chip air gaps). The whole system may also become smaller and more compact. Tung et al. demonstrated the use of integrated fibers to collect light from multiple angles, an important feature of flow cytometry to help enable multi-parameter detection [45]. Exploiting the ability to put a large angle between the illumination axis and the detection line can help minimize the intensity of light scatter reaching fluorescence detectors. The approach can be modified to instead collect light scatter from several angles. For example, orthogonal light scatter could now be collected, something very difficult to achieve by off-chip optics. Chips with integrated illumination and detection lines seemed to offer greater possibility for mass-production and utility, eliminating the problem of aligning off-chip optics after chip replacement or system movement.

Waveguide and fiber based systems can help reduce the size of the device and facilitate interfacing, but their gains have some limitations. The lack of a collimated interrogation source is problematic for uniform, localized sample excitation; similarly, the use of fibers or waveguides for light collection doesnt provide the same localized, high NA light collection used in traditional benchtop flow cytometers [45]; most of the light collected by a fiber originates from locations other than the cell. Indeed, many of these problems were pointed out some years ago in the context of fiber-based optical systems for benchtop cytometers [12]. The issues of cladding mode propagation, high levels of background light collection, and fluorescence induced in the materials are just as applicable to the above-mentioned fiber- and waveguide-based miniaturized systems as they were to a bulk system.

C. On-Chip Lenses

In recent years, research has been working to more exactly replicate the flow cytometry optical system on a chip by including some form of lenses to allow for light control. On-chip lenses could allow for a collimated interrogation beam, yielding more reproducible results and reducing cross-talk. The levels of background light collection can be greatly reduced with a properly designed optical system. Additionally, lenses can be used to increase the numerical aperture of light collection from the cell, further improving device sensitivity. In fiber- and waveguide-based systems, the diverging light path requires the use of a lens for collimation.

Many researchers have focused their attention on the chip for improving the optical system performance. The first integrated lenses in microfluidic flow cytometry were seen on the interrogation line. Camou et al curved the face of the fiber sleeve, almost like a lensed fiber, to create lenses with a radius of curvature as high as 70 μm with a aperture the width of an optical fiber [55]. This idea was explored further in microfluidic chips for absorbance measurements by Ro et al., giving a clear demonstration (see Figure 5) of the advantageous collimating effect of lenses on fiber ends, but also pointing out the dependence on relative fiber position [56]. Wang et al. demonstrated a device employing the more performance-stable waveguide analog of this idea [57]. In this work, the end facet of a waveguide was given lens-like curvature to help localize the excitation beam in the fluidic channel. The authors measured light scattering CVs of 26.6–29.7%. Each of the above works helped to localize the excitation beam in the fluidic channel, recognizing and acknowledging the critical role of that the optical system plays in the functionality of a flow cytometer.

Seo and Lee took the on-chip lens concept to the next level, employing multiple lenses to shape the illumination beam in order to maximize the resulting fluorescence intensity of a sample in a microfluidic channel [58]. This work demonstrates an important improvement: the use of 'free space' optics on a microfluidic chip. The lenses are not tethered to the end of a fiber or waveguide; they can be placed anywhere on the chip. With such a technique, researchers can start to recreate an optical system on a chip. Godin et al demonstrated a fluid-filled lens system integrated with waveguides (see Figure 6), offering the benefit of reduced reflection at the interface and the possibility for higher numerical aperture light collection [59].

It should be noted that creating lenses for light collection systems pose a slightly harder problem than lenses for interrogation systems due to the potential for large losses of light in the vertical dimension after only a short travel distance (e.g. across the microfluidic channel). For this reason, most systems employing on-chip lenses for light collection also involve a form of slab-waveguiding. In the work by Wang et al., light traveled in waveguides made of SU8 or in water, cladded by a either air, glass, or PDMS (depending on location), however, these lenses were physically tied to the location of the fluidic channel [57]. Godin et al. [59], following earlier works by Lien et al. [51], employed a PDMS-core, PDMS cladded system for 'free-space' on-chip optics (Figure 7). This technique allows for a robust device with different optical layers to be created by well-known PDMS-PDMS bonding techniques that yield a permanently bonded interface. With a slab waveguide, in-plane lenses can be placed anywhere on the chip without the concern of additional vertical light loss. This enables lenses to be used in the detection systems as well as in the interrogation system [60]. As mentioned before, this helps to reduce background light collection levels and increase the collection numerical aperture with respect to the cell being interrogated, critical concerns for demonstrating a
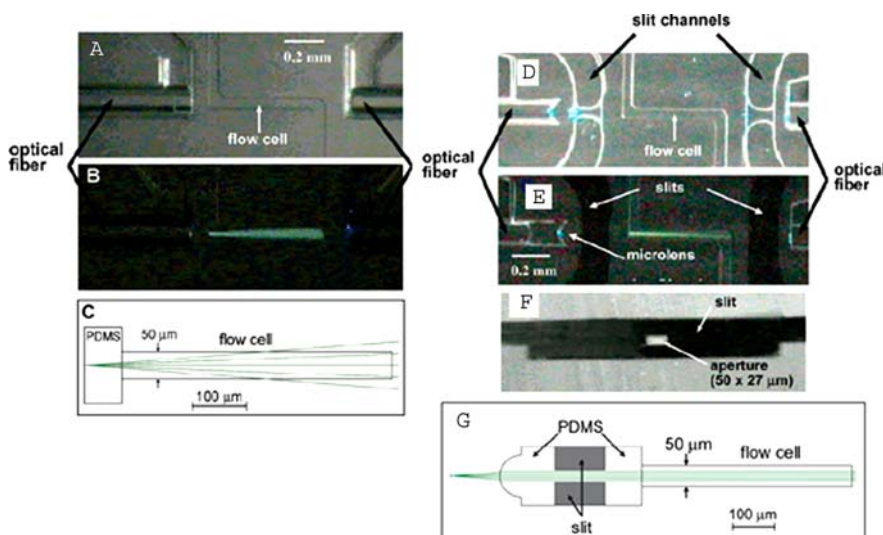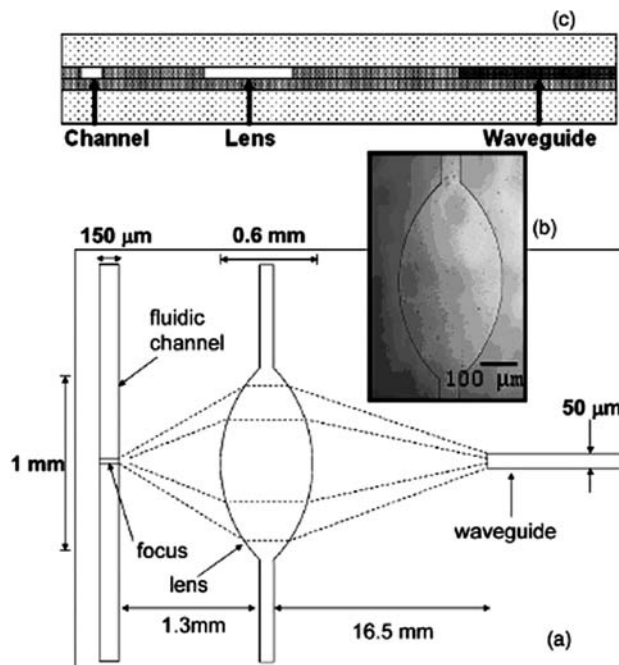

Figure 5 (online color at: www.biophotonics-journal.org) Left: Ro et als Flow cell (a) illuminated only by a fiber optic (b), exhibiting divergence predicted by ray-tracing simulations (c). Right: A similar flow cell (d) with a lensed air space (microlens) at the end of the fiber. The microlens acts to collimate the light from the fiber (e) with the help of stray light blocking by the aperture (f), as expected from ray tracing simulations (g). The resulting smaller, more uniform interrogation beam would be desirable for uniform, localized excitation in flow cytometry chips. Reprinted with permission from [56]. Copyright 2003 American Chemical Society.
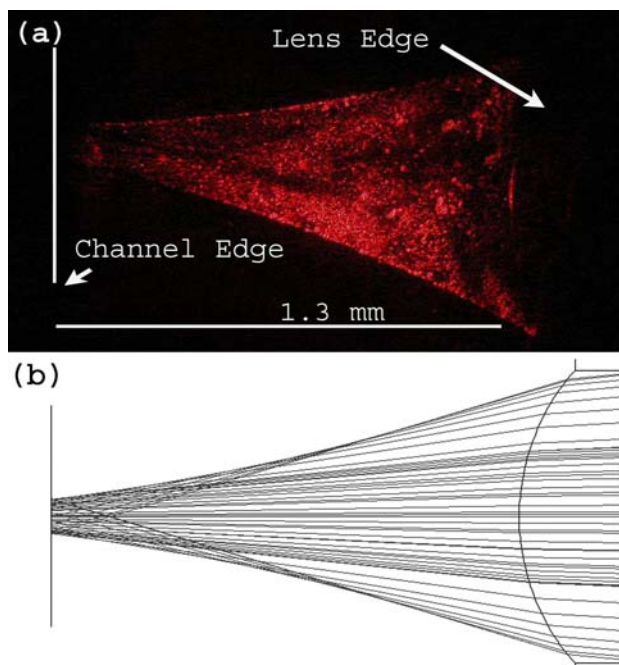
Figure 6 (online color at: www.biophotonics-journal.org) Comparison of (a) an experimental image of a cylindrical lens in PDMS focusing light and (b) the simulated effects of the fluid-filled lens in PDMS [59]. Reprinted with permission from J. Godin, V. Lien, and Y. H. Lo, Applied Physics Letters, 89, 061106 (2006). Copyright 2006, American Institute of Physics.

Figure 7 Schematic of a polymer chip (a) including a waveguide and a fluid filled lens (b). A side view (c) shows the three-layered device, with darkest shading representing the highest refractive index PDMS and the lightest shading representing the low-index cladding layers [59]. Reprinted with permission from J. Godin, V. Lien, and Y. H. Lo, Applied Physics Letters, 89, 061106 (2006). Copyright 2006, American Institute of Physics.

BsoC due to the potentially dim scattering and especially fluorescence levels from actual cells. For this work, CVs of 10–15% were demonstrated for 4.8 μm polystyrene beads, a significant improvement over previous lensless light collection on microfluidic cytometry chips, where CVs of 20–30% are typical [22, 57]. The design is currently being extended to include even smaller lenses and many more of the components and layout of a tradition cytometer (see Figure 8): a collimated interrogation beam on the order of a few tens of microns in diameter, a forward scatter line with a beam stop to block the interrogation beam, and an orthogonal scatter collection line. This fabrication system should also allow for the design of large NA lens systems for the collection of fluorescence, completing the suite of optical capabilities that users expect of a benchtop cytometer. As Figure 8 demonstrates, complex, highly-integrated fluidic and photonic systems can be easily constructed with this simple fabrication method.

In addition to such two-dimensional systems, some attempts have been made to fabricate three-dimensional lenses [61–62]. The authors used a diffusion mask to scatter the collimated light from a traditional mask exposure system. The resulting features had sidewalls that curved inwards, thus the molded lenses were convex in nature. This technique

helps to keep light from escaping above or below the optical path; however the curvature of the lens is not currently well-controlled with this approach. With further development, three dimensional lenses could reduce or eliminate the need for a slab-waveguided system, and may be able to increase the numerical aperture of collection in the vertical dimension.

On-chip optics do not come without a downside, however. Each interface presents some scattering and reflection losses. Considering unpolarized rays of near-normal incidence, the Fresnel reflection coefficient $R \approx [(n_1 - n_2)/(n_1 + n_2)]^2$ per surface. Without the availability of antireflection coatings, reflection losses can start to become substantial in multi-lens systems, especially for light collection lines. Reflection losses can be mitigated by the use of immersion-type lenses, i.e. low index contrast or weak lenses. In addition, careful attention must also be paid to the issue of sidewall roughness in order to maintain performance. High-resolution transparency masks must be replaced by higher quality, higher costs masks, such as the traditional electron-beam written chrome mask, in order for feature roughness to stay smaller than the Marechal Criterion of $\sigma_{rms} \leq \lambda/14$ (e.g. rms roughness under 35 nm for 488 nm light) [63]. Additionally, typical microfluidic
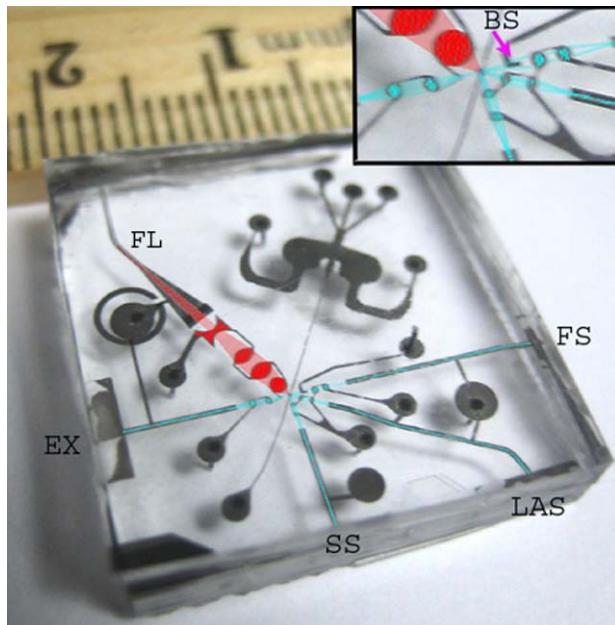
Figure 8 (online color at: www.biophotonics-journal.org) Early prototype of a microfluidic cytometry chip including waveguides and lenses for an excitation source (EX), a forward scatter collection line (FS) including a beam stop (BS), a side scatter collection line (SS), a large-angle scatter collection line (LAS), and a line for fluorescence collection (FL) (unpublished). The seamless integration of fluidic and photonic elements is accomplished by simple microfabrication techniques [60].

chip feature depths are quite large by microfabrication standards (~ 50–$100\,\mu$m), so maintaining smooth, optical-quality sidewalls for this depth can pose quite a challenge. Seo et al. reported roughness ~ 100 nm for their silicon mold sidewalls after a DRIE fabrication process. They were able to further reduce this roughness to 20 nm using a wet etching process [64]. Molds created by SU8 polymer can have sidewall roughness down to 25 nm or below as well [65]. Careful attention must be paid to ensure that sidewalls are not just smooth, but are also vertical and exhibit sharp corners. Rather than create physically smooth sidewalls, the previously-mentioned L^2 lens mitigates the issue of surface roughness by using a continuous flow fluidic lens whose shape is controlled by a sheathing fluid, which is index-matched to the substrate [54]. This effectively masks the sidewall roughness, and the lens sidewall becomes the much smoother fluid-fluid interface.

D. Beyond Lenses

A few groups have started to venture even a bit further than lenses, creating an even broader optical toolbox that can further improve the performance of microfluidic flow cytometry chips. Apertures have been demonstrated by filling PDMS channels with black ink [54, 56]. Apertures and beam blocks play an important role in background and stray light reduction in traditional flow cytometers, thus the ability to implement these features in microfluidic flow cytometers will be an important step in attaining performance on par with the benchtop device [66].

Kou et al demonstrated prisms for beam steering [67]. Following the concept of spectral flow cytometry [68], the use of similar microfabricated prisms or perhaps gratings could be envisioned as the dispersive elements for the implementation of compact, multi-color detection systems. Integrated filters have also been demonstrated in PDMS-based devices using dye-doped polymer to create absorption filters [46, 69]. Hoffman et al demonstrated Sudan II-doped PDMS long pass filters with >80% transmission above 570 nm and <.01% transmission below 500 nm [69]. They also note negligible autofluorescence, a very important consideration for fluorescence detection devices. Bliss et al extended the idea of Sudan-doped PDMS to create 'wavelength-selective' waveguides: waveguides that absorb the illumination light while passing the excitation light. Transmission above 570 was high (near 100%), while transmission dropped to 3–11% for wavelengths below 500 nm. Tunable filters based on flow of absorbing fluids have been described as well [70].

Some researchers have taken integration even a few steps further, integrating lasers and detectors onto the chips as well. Balsev et al. explored the possibility of a fully-integrated chip: laser, fluidics, and detectors all on a single silicon chip with SU8 features [71]. A number of researchers have demonstrated means of creating on-chip lasers [67, 72]. Dye lasers in particular are favored in microfluidic systems due to their materials system compatibility. These lasers offer the benefits of compactness, low power consumption, and wavelength tunability. Unfortunately these lasers still require an optical pump source; however, diode lasers may be a good candidate for a pumping source as they continue to become smaller and higher-powered.

Researchers have also been considering the way in which data is collected in an attempt to improve the acquired signal in microfluidic flow cytometry. In particular, if the sensitivity of the collected data can be enhanced, researchers may be able to sacrifice some sensitivity (and thus cost or size) of the detectors; namely to switch from the use of PMTs to photodiodes. Additionally, such sensitivity enhancements would be helpful even for the more sensitive APD-based detection systems to reach higher operating standards, for example in low-intensity fluorescence measurements. Lien et al exploited the ability to readily create an array of waveguides in a micro-
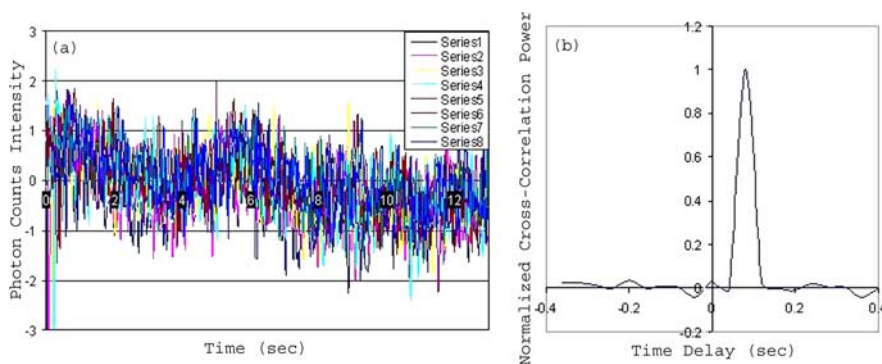
Figure 9 (online color at: www.biophotonics-journal.org) Using time-delay cross-correlation, 8 noisy signals (a) are shifted and integrated to yield a single large peak (b) showing that a single 1 μm fluorescent bead has passed [73]. © 2005 IEEE.

fluidic chip to perform multiplexed data collected, and to further employ time-delay cross-correlation for signal enhancement [73]. In this device, each sample by passed eight equally-spaced sets of interrogation and collection waveguides, yielding eight detected signals, as shown in Figure 9. Using the known time delay between expected signals, cross-correlation was performed, yielding great improvement the signal-to-noise ratio of the data. Signals invisible to the eye were readily extracted with excellent clarity. In another approach to enhancing the S/N ration, Tung et al. modulated their two laser sources at 100 kHz and used a lock-in amplifier with photodiodes to extract their signal from a very noisy background [45]. Their approach obtained 25–35% fluorescence CVs in a fiber-based microfluidic device.

For a microfluidic cytometer to truly become a viable alternative to a benchtop cytometer, it must be capable of meeting the current performance expectations of a benchtop cytometer. The importance of inclusions such as true forward scatter (rather than extinction) or traditional orthogonal side scatter should be considered for the intended application of the device. In addition, the eventual limitations of important criteria such as optical sensitivity, throughput, or sorting efficiency must be addressed for each approach considered. Eventually, it is the end-users who will judge the value of the device, and thus it is the expectations of the end-users that researchers should have in mind.

III. Cell Sorting Techniques

As researchers' interests in studying single cells (e.g. detection and isolation of rare stem cells and circulating tumor cells [74–75] and cellular metabolism [76–77]) grow, a cell sorter capable of sorting single cells with high throughput, purity, and cell viability has become indispensable for a microfabricated flow cytometer. The cell sorter typically operates under continuous flow separation [22]. This entails screen-

ing of individual cells upstream from the sorter, which provides information to a feedback mechanism to activate the sorter downstream such that single targeted single cells are deflected in some manner towards a collection chamber. In recent years, along with improvement in microfabrication technology, various sorting modules have emerged. Among these modules, the most widely used sorting actuations employ approaches involving electric, magnetic or hydrodynamic forces. The following sections will primarily focus on these advances, considering both their limitations and advantages for cell sorting.

A. Electric Field-Based Sorting

Manipulation of particles/cells based on electric fields has been one of the most widely used methods in microfabricated sorters. Advances in microfabrication technology enable microelectrodes (e.g. platinum or gold electrodes) to be embedded or flanked between two substrates (i.e. one layer with patterned microfluidic channels and another layer to serve as a capping) that extend out to the exterior environment, where DC or AC voltages can be readily applied. Depending on the nature of the application, both homogeneous and inhomogeneous electric field can be applied to sort particles/cells of different properties (e.g. neutral, charged, and polarizable particles).

In one of the first demonstrations of a microfabricated flow cytometer by Fu et al., electroosmotic force was employed to direct a suspension of *E. coli* to the designated output reservoirs [78]. Electroosmotic flow is induced by the migration of charges as voltage is applied between two outlets [79]. In Fus work, sorting of *E. coli* was based on flow switching (electrokinetic switching) as DC voltages were applied between collection/waste outlets and sample inlet. A throughput of ∼20 cells/s was reported, well below the commercial bench-top cytometer speeds (10,000 cells/s or faster). In a similar approach, L. M. Fu and coworkers sorted red blood cells by means
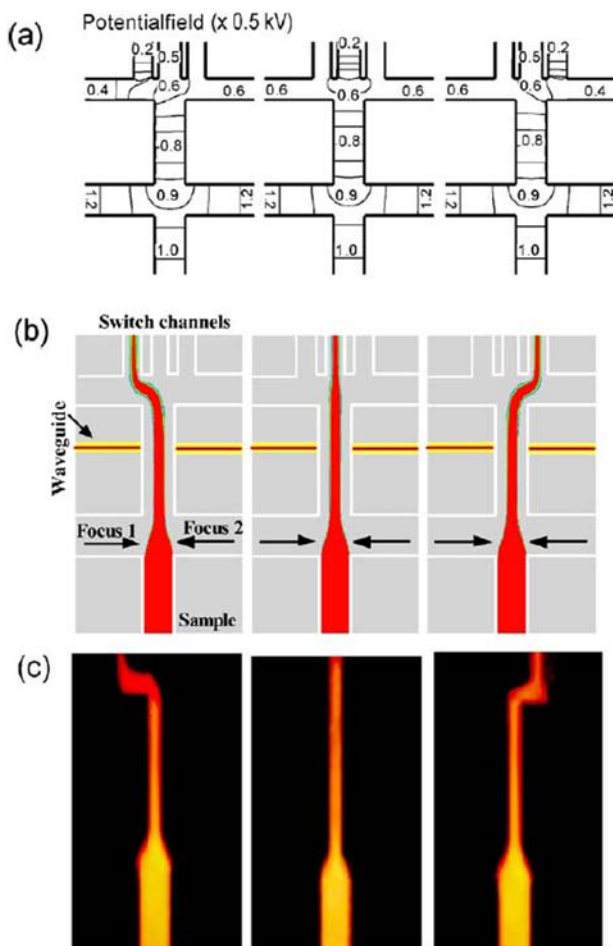
Figure 10 (online color at: www.biophotonics-journal.org) a) Electric potential contour at 2 : 1 focusing ratio (e.g. ratio of voltage applied to focusing channel to sample channel). b) and c) show the numerical simulation and experimental results of the flow switching phenomena. Reprinted from [80] with permission from Elsevier.

of electrokinetic switching [80]. By changing the relative voltages applied to the outlet channels, the sorter can achieve three switching modes (shown in Figure 10), which provide the potential of sorting three different particle/cell types in a given run. In this work, focusing and sorting have both been achieved electrokinetically by applying DC electric fields, but the magnitude of the DC voltages needed ranges from 300–500 V, which is impractically high due to the high power consumption. Also, high electric field not only can cause heating problems but also inflict great damages to cells and thus, rendering cell viability significantly low after sorting. Another electroosmosis-based sorter, requiring a significantly lower input voltage (e.g. 40 V), was demonstrated by Dittrich and Schwille [81]. This system incorporated an electrokinetic-driven flow channel oriented perpendicular to the sample channel. As a hydrodyna-

mically-driven particle enters the Y sorting junction, activation of a perpendicular electroosmotic flow will deflect particle to either side of the output channels (depending on the polarity of the input voltage). Though different colored fluorescent beads could be sorted, the reported throughput was between 0.3–1 beads/sec, limited by the activation time of the electrodes for inducing the electroosmotic deflection flow. In summary, electroosmosis-based sorters are relatively easy to fabricate (insertion of Pt electrode into the inlet/outlet reservoirs) and the operation is relatively straightforward, but they suffer from some common drawbacks including frequent change of voltage settings due to ion depletion [82], electrolysis-induced bubbles at the electrodes surface, low throughput and potentially low cell viability, and high power consumption (e.g. the use of high DC voltages).

Sorting based on dielectrophoresis (DEP) has also become very popular over the years, as the approach can alleviate some of the major limitations encountered by the electroosmosis-based methods such as high power usage, low throughput, and reduced cell viability. Rather than the uniform electric field produced in electroosmosis, DEP exposes particles/cells to a nonuniform electric field by applying AC voltages in ultrasonic regime (i.e. MHz) to the fluid-immersed electrodes. The dielectrophoretic force experienced by the particle within the field can be described by the following equations [83]:

$$F = 2\pi a^3 \varepsilon_1 \, \mathrm{Re} \, (f_{\mathrm{CM}}(\omega)) \, \mathrm{grad} \, (E^2) \tag{1}$$

where a is the radius of the particle, ε_l is the permittivity of the suspending medium, ω is the angular frequency and $\mathrm{Re} \, (f_{\mathrm{CM}}(\omega))$ is the real part of the dipolar Clausius-Mossotti (CM) factor (i.e. $-0.5 < f_{\mathrm{CM}}(\omega) < 1$), where:

$$f_{\mathrm{CM}}(\omega) = \frac{s_p^* - s_l^*}{s_p^* + s_l^*} \tag{2}$$

Here ε_p^* and ε_1^* are complex permittivities of the particle and the surrounding solvent, respectively. When particles/cells experience electric field, they become polarized. Due to the relative polarizability between the solvent and the particle, there is a net movement of particles/cells toward either the high or low electric field locations, depending on the polarizability (see Figure 11). Positive dielectrophoresis **(pDEP)** occurs when the polarizability of the particles is larger than the polarizability of the surrounding fluid (i.e. $f_{\mathrm{CM}}(\omega) > 0$). In this case, particles are attracted to the high electric field region. In contrast, when the solvents polarizability is greater than the particles polarizability, negative dielectrophoresis **(nDEP)** comes into play, causing particles to migrate toward the low electric field region. Since the magnitude of the DEP force is highly dependent on both the size and the polarizability of the particles/cells (refer to
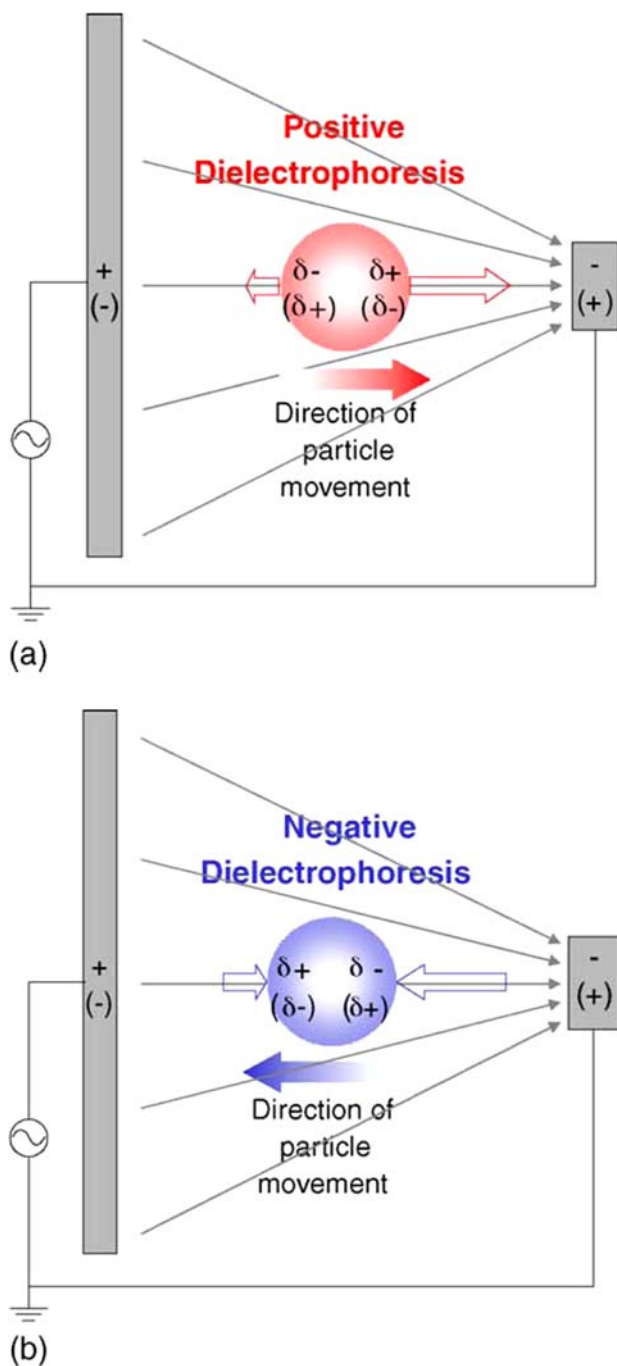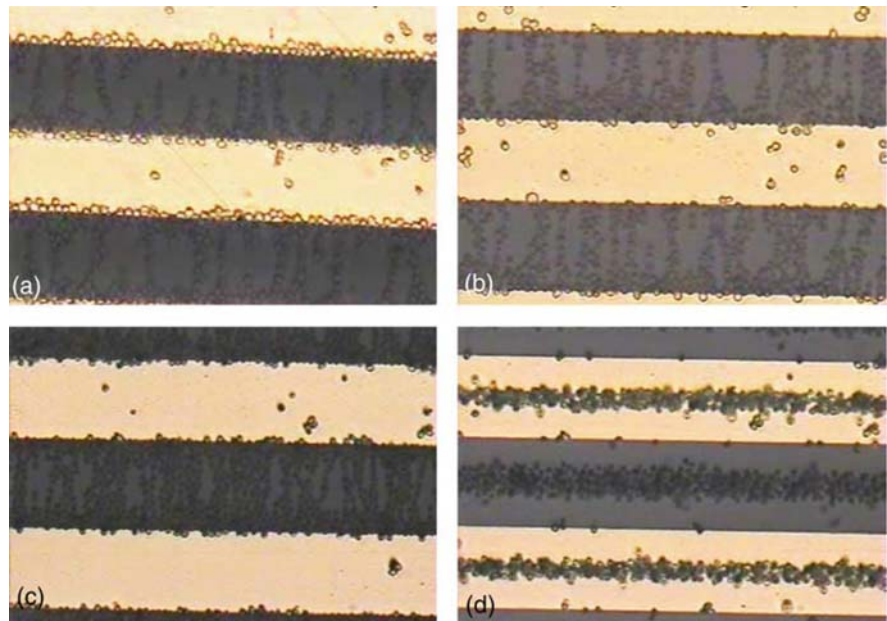
Figure 11 (online color at: www.biophotonics-journal.org) Particles/cells suspended in an inhomogeneous electric field undergoing a) positive dielectrophoresis (pDEP) and b) negative dielectrophoresis (nDEP) will move to regions of high electric field and low electric field respectively. Whether the particles are pDEP/nDEP-activated depend on the relative polarizability between the particle and the surrounding medium. Reprinted from [94] with permission from Elsevier.

Eq. (1)), researchers have been exploiting these characteristics to perform separation and sorting on various types of polymer beads and cells.

DEP-based particle manipulation was first used to funnel and trap single beads/cells by incorporating arrayed posts [84–88] inside the microchip. In early work, Fiedler et al have designed a 8-electrode quadrupole cage to trap (via nDEP) single 3.4 μm latex bead and L929 cells to the center of the cage [84]. Following this work, Voldman et al. have applied arrayed quadrupole DEP trap to hold and isolate multiple single fluorescent cells against continuous pressure-driven fluid flows [85] for up to 2 minutes. By adjusting the operating frequencies (1–20 MHz) and voltage (1–3 V), the arrayed gold posts are able to overcoming flow rates up to 15 μl/min to hold these single cells in place. This method allows researchers to study transient cellular response when exposed to different chemical stimuli. Although DEP-based trapping can provide non-contact isolation down to the single cell level using relatively low power ($<$10 V), it usually requires complex fabrication process and can potentially cause cell damage, as cells are exposed to electric field for an extended period of time.

In addition to cell trapping, DEP-based sorting under continuous flow conditions has been demonstrated by creating obstacles along the flow [86, 89–91] and by quick deflection at the sorting junction [92–93]. By narrowing a 300 μm channel down to 60 μm using a rectangular obstacle, Kang et al. were able to separate 5 μm, 10 μm, and 15 μm particles into two downstream outlets under the influence of nDEP [91]. Unfortunately, most obstacle-based DEP designs require high input voltage (e.g. hundreds of volts), and are therefore not practical in sorting biological agents (due to cell damage). Combining an optical detection system upstream, Holmes et al. designed embedded 2-electrode systems in both T- and Y-junction configurations [92]. The electrodes, which lie perpendicular to the fluid flow, serve to deflect particles into one of the two identical channel outlets, both of which are 75 μm wide and 40 μm high. Operating at 10 MHz with a 20 V peak-to-peak voltage, the system could deflect 6 μm particles at a rate up to 300 particles/s. However, under automated sorting (e.g. a closed loop control system), a throughput of only 10 particles/s was demonstrated. Although the authors claimed the system can sort up to 1,000 particles/sec, the potential challenge of overcoming the increase in hydrodynamic drag force at increased flow rates with the relatively small DEP force is not addressed.

With the advent of micro DEP-activated cell sorting (DACS) technology in recent years, the need for closed-loop electronic implementation can be eliminated. Doh and Cho fabricated a system consisting of three inlet and outlet channels with a DEP separation region in between. This region consisted of three fluid-aligned 200 Å/1000 Å Cr/Au electrodes embedded inside the 50 μm high fluidic channel (e.g.

Figure 12 (online color at: www.biophotonics-journal.org) Bands of yeast cell aggregations under 8 Vp-p at sinusoidal frequencies of a) 10 kHz and b) 5 MHz for viable yeast cells and c) 10 kHz and d) 5 MHz for nonviable yeast cells. The bright and dark regions are electrodes and glass substrate respectively, and the cells are immersed in a 5 μS/cm buffer fluid. Reprinted from [94] with permission from Elsevier.

in direct contact with fluid) [94]. The design is implemented for separating a mixture of viable and nonviable yeast cells in hydrodynamically-driven continuous flow. Since viable and nonviable yeast cells demonstrate a different dielectrophoretic response (i.e. either nDEP or pDEP, respectively) at different electric field frequencies and medium conductivities, the authors were able to separate viable yeast cells from nonviable yeast cells (see Figure 12) at a maximum throughput of 1300 cells/sec with 97% purity in the viable fraction and 70% in the nonviable fraction. Under 5 MHz frequency in a 5 μS/cm fluid medium, viable/nonviable cells which experience pDEP/nDEP would move to a area of high/low electric field, resulting in spatial separation as the cells approach exit channels. Similarly, by placing 200 nm arrayed platinum electrodes perpendicular to the fluidic flow, Braschler et al. have also separated viable and nonviable cells with a purity of nearly 100% [95]. In addition, the authors have also enriched red blood cells infected with B. bovis from a 7% infected mixture to a 50% infected mixture. The inability to obtain higher purity is due to high variability of dielectric properties for non-infected blood cells.

By conjugating polystyrene beads to rare bacteria that express specific surface markers, Xiaoyuan Hu et al. were able to amplify the difference in DEP response between targeted and non-targeted bacteria for DACS [96]. The 300 nm Au electrodes serving to deflect cells under nDEP are situated at an angle of 15° relative to the direction of the flow. As bead-labeled bacteria encounter the electrode, the nDEP force (~388 pN) experienced by the bacteria will overcome the hydrodynamic drag force (~368 pN), resulting in sorting of targeted cells into the collec-

tion channel (Figure 13). Using this method, the authors achieved a throughput of 10^4 cell/s, ~95% recovery, and 250-fold enrichment after 2 rounds of DACS. This is the first DEP sorter exhibiting throughput comparable to a bench-top FACS. In the authors most recent work, they developed a two-stage DACS to screen E coli cells that display peptides which bind to antibody from a library of 5×10^8 different clones at a throughput of $>10^8$
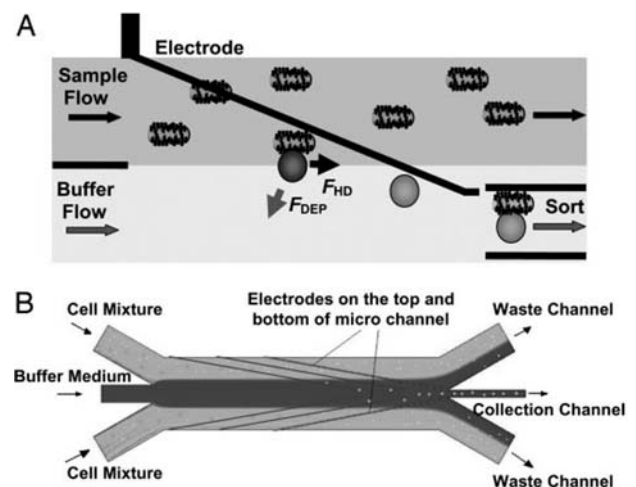
Figure 13 Sorting mechanism for the DACS. A) Bead-labeled cells experience significantly higher nDEP force than non-labeled cells and therefore, can overcome hydrodynamic drag forces resulting in transversal movement down to the collection channel. B) Schematic view of angled electrodes, inlet channels (e.g. buffer fluid sandwiched by two sample channels), and outlet collection and waste channels [96].

cells/h [97]. The method requires additional bead-labeling process (yield was not reported) and may cause cell damage due to prolonged electric field exposure, it does provide a continuous, contactless, low-powered, DEP-activated separation with high purity and throughput comparable to commercial FACS.

B. Magnetic Sorting

Magnetic cell sorting via on-chip devices has received relatively little attention. Cell sorting by applying magnetic field has been tried by some research groups. In magnetic sorting, cells of interest are labeled with magnetic beads first and they are separated from the sample flow by magnetic field. Magnetic labeling of biological cells or particles with magnetic nanoparticles is performed by attaching magnetic particles to the cell surface [98] or by introducing them into the cell [99].

It is reported that paramagnetic beads can form an immuno-capture 'bed' in order to isolate rare cells from blood. Some groups have utilized magnetic beads in microfluidics devices for chemical and biological reactions. Those magnetic beads beds were successfully applied to dynamic DNA hybridization [100] and mRNA isolation [101] within a microfluidics devices. The sample particles were stopped in laminar flow by an external magnetic field and the reaction was performed on the particle bed.

N. Pamme et. al. demonstrated the continuous sorting of living biological cells, mouse macrophages, and human ovarian cancer cells (HeLa cell) by free-flow magnetophoresis (i.e. without stopping sample particles) [102]. Because the sample particles flow continuously inside of the microfluidic channels, the chip operation is simplified; more importantly, throughput and cell sorting efficiency are greatly improved. In this work, the biological cells were internally labeled with magnetic nanoparticles. A permanent magnet, or electromagnets, were placed beside the microfluidic channel. The microfluidic channel had 16 inlet channels and 16 outlet channels. The magnetic particles are introduced throughout rectangular laminar flow chamber (Figure 14) [103]. A magnetic field is then applied perpendicular to the sample flow direction. Magnetic particles, such as the labeled cells, migrate into this field and thus deflected from the direction of laminar flow. Particles deviate from the laminar flow according to their size and magnetic susceptibility, so they are successfully separated not only from non-magnetic material but from other magnetically-labeled cells as well. The magnetically-labelled particles were not generally sorted into a single channel; they were often distributed over several channels, making precision sorting difficult.
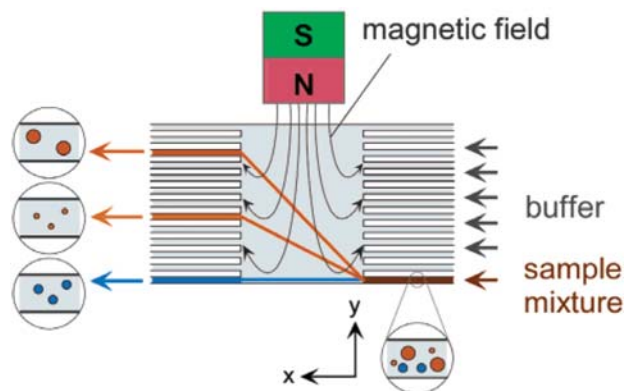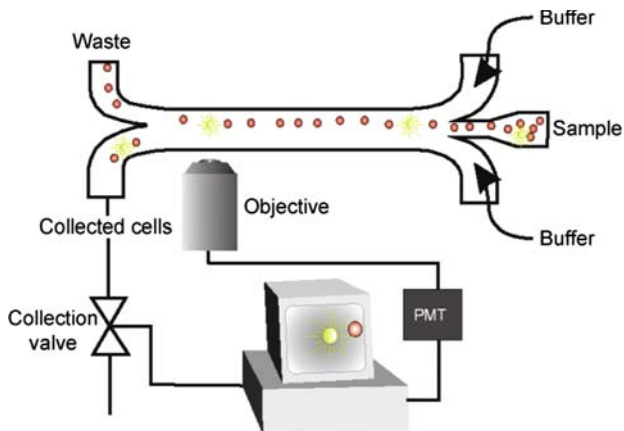

Figure 14 (online color at: www.biophotonics-journal.org) Schematic of free-flow magnetophoresis. Particles in the magnetic field deviate from their original directions as a magnetic field is applied in the direction a laminar flow. This deviation depends on the size and magnetic susceptibility of each particle [103].

Ingber et. al. investigated high-gradient magnetic field concentrator (HGMC), which pulls biological cells in one laminar flow to another flow without washing steps by simply applying a local magnetic field gradient [104]. They used a soft magnetic material (NiFe) to facilitate switchable control of the sorting operation. A local magnetic field gradient magnetized the HGMC, and the magnetic particles were pulled from the initial flow path into another flow stream for collection, cleansing the initial fluid as well. One of the advantages of HGMC device is its ability to generate a large magnetic force with simple structure, therefore inducing large deviations for particles of interest and enabling accurate, simultaneous sorting for multiple particles.

C. Hydrodynamic Sorting

Sorting using hydrodynamic force can be a good alternative to electric or magnetic based sorting, as issues such as buffer incompatibility (i.e. the required usage of buffer with specific conductivity), ion depletion, and cell damage due to electric fields or magnetic labeling can be readily resolved. In addition, since hydrodynamic-based sorters are usually fluorescence-activated (i.e. cells are labeled with fluorescent surface markers), the method represents a more generically applicable approach in that it does not sort based on cell properties (e.g. index of refraction, size, dielectric property, etc). The implementation of these sorters often involves external check valves [36, 105], integrated PDMS-based valves [106–108], or external syringe pumps [109–110] to achieve flow switching. In one example, Wolff et al. attached a high-speed external valve (2.5 ms response time) to

Figure 15 (online color at: www.biophotonics-journal.org) Schematics of high-throughput μFACS. Activation of external collection valve (i.e. triggered by upstream fluorescent detection signal) draws out a fixed fluid volume, which contains the targeted cells, into the collection channel [36]. *Reproduced by permission of The Royal Society of Chemistry.*

the collection outlet to sort rare fluorescent beads from chicken red blood cells (Figure 15). A throughput of 12,000 cells/s (comparable to bench-top flow cytometer) and an enrichment of 100-fold were reported, though the purity of the sorted sample is low [36] (i.e. nontargeted cells are collected along with
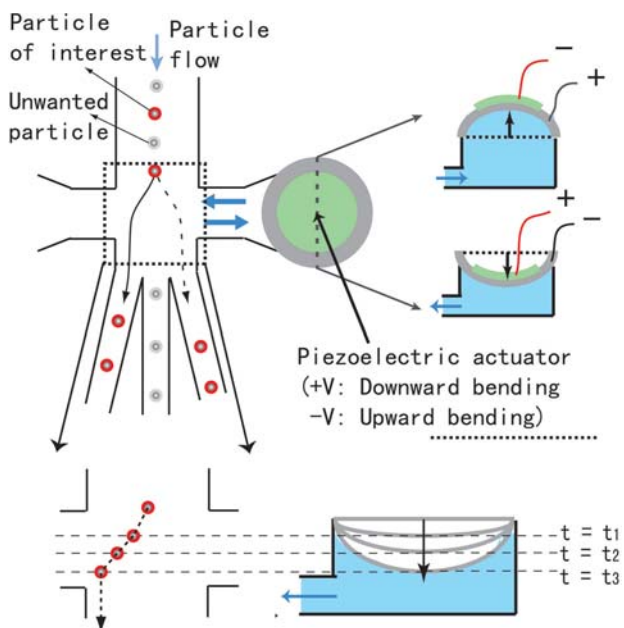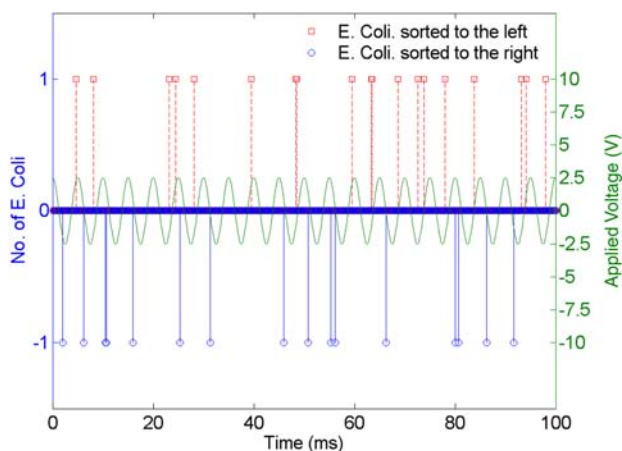

Figure 16 (online color at: www.biophotonics-journal.org) Working principle of the piezoelectric (PZT) actuation-based sorter. The particles/cells are deflected down to the collection channels (left or right channels) as PZT actuator bends upward/downward. The transverse movement of particles is caused by the drag force of the fluid displaced by the PZT actuator as it bends (unpublished).
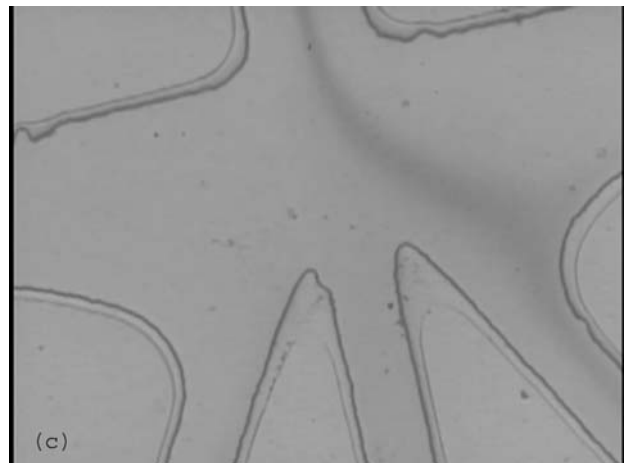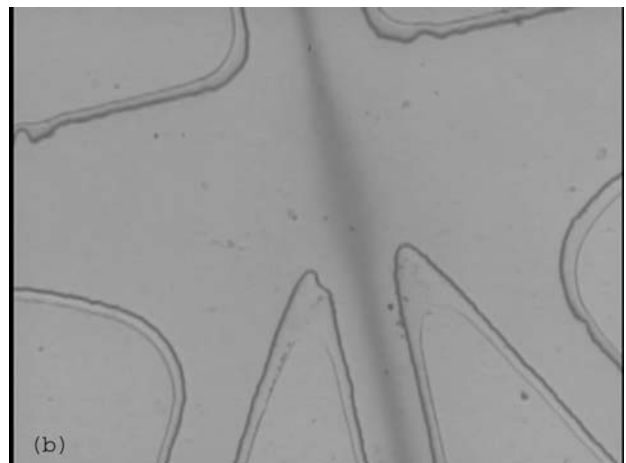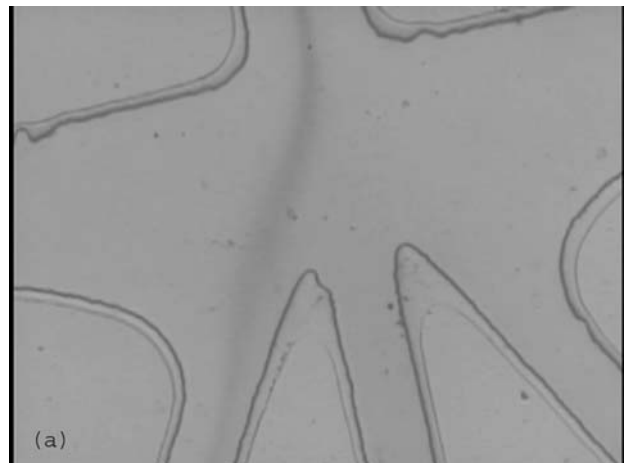
Figure 17 Images showing the flow-switching capabilities of the PZT-based sorter. The flow stream (Rhodamine 6G) switches (a) to the left and (c) to the right as PZT actuator becomes positively (e.g. downward bending) and negatively biased (e.g. upward bending), respectively. During the non-ramping state (i.e. the actuation-off state), the flow stream returns (b) to the central region and exits down to the waste channel (unpublished).

the targeted cells). Flow switching can also be controlled through fluid injection by using a syringe pump, as demonstrated by Krüger et al. As the syringe pump is activated, plugs of nano-liter fluid are injected in an X-junction, causing a temporary shift of stream flow from waste channel into the collection channel [110]. The drawback of this method is the slow mechanical response of the syringe pump (i.e. a switching cycle of $\sim$200 ms), suggesting that the throughput of the system will be very low as well ($<$0 particles/sec). Fu et al. demonstrated an integrated valve sorter, where cell sorting is performed by opening or closing the PDMS-valve pneumatically at a pressure of about 60 kPa [106]. The throughput ($<$50 cells/s) is limited by the mechanical compliance of the valve, which has a theoretical response time of $\sim$5 ms [107]. In a very recent development, rather than using pumps and valves with limiting response times, a piezoelectric (PZT) actuator is integrated on-chip (in place of a membrane) to manipulate flow streams based on a pushing and pulling mechanism (Figure 16) [111]. As the PZT membrane bends downward and displaces fluid, the particle entering the sorting junction will be deflected to the left to enter the lefthand collection channel. During the non-ramping state, particles will travel straight down, into the center waste channel. Fluid stream deflection due to PZT actuation is vi-

sualized in Figure 17. The magnitude of the deflection can be precisely controlled by the input voltage, showing the potential to extend the architecture (e.g. from 3-outlet to 5-outlet system) to sort cells of multiple types. In addition, the device has been demonstrated to deflect *single E. coli* cells into the collection channel at a rate of $\sim$330 cells/s under 200 Hz actuation frequency and 6 V peak-to-peak AC voltage (Figure 18). Compared to other sorters, this design has the advantages of low power consumption ($<$10 V), simple fabrication process (i.e. bonding of PZT actuator to the substrate), and property-independence (e.g. properties of cells or surrounding fluid) sorting. Furthermore, since PZT actuators are designed to operate at relatively high frequencies (a resonant frequency range of 1–10 kHz in this work), the sorter has the potential to sort thousands of particles per second (at the single cell level), eliminating the problem of slow mechanical response time.

Conclusion

Microfluidic devices offer a small, simple platform for flow cytometry that has excellent ability to integrate current components as well as accommodate future changes and improvements. There are a number of hurdles that must be overcome to create a functional device. Materials choices can create a number of difficulties. While PDMS is often the material of choice for researchers, it is known to have issues with fluid and chemical absorption. In addition, while replica molded devices show the potential for mass-production, especially relative to serial processes like photolithography, there are currently very few, if any, production-scale facilities. This of course poses a problem for fabricating and selling devices at a low cost. Keeping the final package small also poses a problem; a small chip is very nice, but lasers, detectors, fluidics, and electronics can make the final device considerably larger.

To become a practical instrument, such devices must be shown capable of performing the tasks of a traditional cytometer with sufficient sensitivity and resolution to satisfy the end user. On the detection side, this means demonstrating truly multi-parameter devices with CVs that can begin to rival a benchtop cytometer. This means employing high-quality optical systems, on- or off-chip, along with three-dimensional sheath flow and a stable, well-shaped light source. On the cell sorting side, this means achieving both high throughput (1–10 kHz operation) while maintaining high reliability (sorted sample purity $>$90%). Additionally, in the case of low-cost cytometry, researchers should be attentive to the eventual need for a highly user-friendly interface. If microfluidic cytometers are intended to be deployed to re-

Figure 18 (online color at: www.biophotonics-journal.org) Results from the sorting of single E. Coli. cells at 200 Hz frequency under 5 Vp-p actuation voltage. The peaks are obtained by identifying cells visually as they are sorted to the left or right collection channels. A total of 330 cells are visually counted in 1 sec. Note that some rare peaks which appear denser mean that two cells have exited a particular collection channel at roughly the same time. Also note that time at which cells are sorted to the left or right correspond to the downward or upward (bending) ramping state; that is, these events correspond to the upward or downward slope of the applied signal on the PZT actuator, consistent with the proposed mechanism of sorting (unpublished).

mote, resource-poor settings or purchased by individual research laboratories, the machines will need to be easy to operate, requiring minimal training. They must, therefore, exhibit reliable and consistent performance; for example, not requiring changes in operating conditions for sorting different sample types. Additionally, the benefits and drawbacks of integration must be considered each time a component is added to the chip. The added cost of the component, such as an on-chip laser or filter, may or may not be worthwhile to the end user, and further may affect the consistency of performance from chip to chip. Tradeoffs in sensitivity and resolution must also be considered for the application in mind.

The development of a microfluidic flow cytometer may be the advance that brings a cytometer to every research lab, allowing for faster discovery and understanding in areas such as cancer research, drug development, and genetics. Low cost, portable devices could allow for HIV monitoring in remote areas of Africa and Asia, helping antiretroviral drugs make their way to patients in need. Low cost microfluidic devices could further help patients in affluent countries to receive faster test results, and may reduce the amount of blood needed for testing. Microfluidic cytometry chips could eventually integrate reagent mixing stages for rapid, reliable labeling, or cell culture stages for bacterial and fungal studies. For the same reasons that microfluidic photonic devices could revolutionize cytometry, these same technologies hold great promise to revolutionize the fields of biology, chemistry, and medicine. Individual cells or small-volume reactions could be studied in entirely new and detailed ways using small, portable devices affordable to any researcher in any location. The technologies are emerging to create a new class of equipment that holds the potential to be cost effective, portable and massively parallelized. These technologies must be fine-tuned and developed towards meaningful applications, looking both towards improving upon todays devices and also towards finding new technologies to which the integration of microfluidics and photonics can be applied.

Jessica Godin received her B.S. degree in Applied & Engineering Physics from Cornell University in Ithaca, NY in 2004. She received an MS in Applied Physics from the University of California, San Diego in 2006, where she is now pursuing her Ph.D. in the department of Electrical and Computer Engineering. Currently, she is developing an on-chip optical system for compact flow cytometry and other lab-on-a-chip devices. Her research interests include flow cytometry and other means of single-cell analysis, as well as general optofluidic devices.
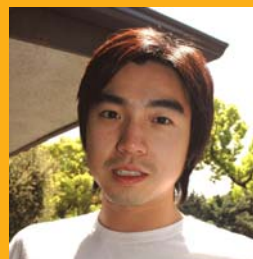
Chun H. Chen has received B.S. degree from University of California, Berkeley in 2003. Currently, he is studying his Ph.D. at University of California, San Diego, in the bioengineering department. For his current research, he is working on developing a high-throughput microfluidic sorter using piezoelectric-based technology that can be applied to cancer diagnostics, genetic study of rare bacterial cells, and isolation of stem cells.

Sung Hwan Cho received the B.S degree in Materials Science and Engineering from Seoul National University, Seoul, Korea, in 2004 and received the M.S degree in Materials Science and Engineering, in 2006, from University of California San Diego, La Jolla, USA, where he is currently working toward his Ph.D. degree. He joined Professor Yu-Hwa Los research group in 2006 and has been working on microfluidic lab-on-a-chip sorting devices and polymer lenses. He is also interested in designing an integrated opto-fluidic system on a polymer-based chip.
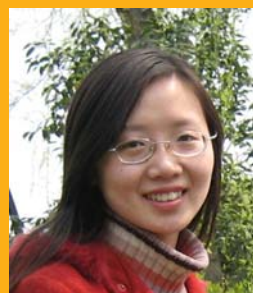
Wen Qiao was born in Nanchang, China, in 1984. She received her B. Sc. Degree in Optics from Tianjin University, China, in 2005. Then she became Ph.D. candidate at Zhejiang University, China. She is now doing doctoral work at University of California, San Diego as a visiting scholar. Her current research interests include fluidic lenses, super-human vision, and microfluidic devices.

Frank Tsai is currently pursuing his Ph.D. degree in University of California, San Diego (UCSD). He received his BS and MS degree in Electrical Engineering from National Chiao-Tung University, Hsinchu, Taiwan, in 1999 and 2001 respectively. From 2001 to 2005, he worked as an engineer in Computer and Communication Research Laboratory, Industrial Technology Research Institute, Hsinchu, Taiwan. His current research interests include microfluidics and bio-inspired fluidic lens.

Yuhwa Lo received his Ph.D. in electrical engineering from UC Berkeley in 1987. He worked at Bellcore (Telcordia) as a technical staff member from 1988–1990, and became an assistant and then associate professor of Cornell University from 1991 to 1999. He became a professor of UCSD in 1999 and has been the director of the Nano3 Facility (Nanoscience, Nanoengineering, and Nanomedicine) since 2005. Currently his research interests are in bio-imaging, bio-sensing, nano-photonics, and single-photon detectors. He has more than 300 publications and been granted 16 patents. He is a fellow of the Optical Society of America and the IEEE.

References

[1] H. Chen and J. C. Meiners, Applied Physics Letters **84**, 2193 (2004).

[2] D. J. Beebe, G. A. Mensing, and G. M. Walker, Annual Review of Biomedical Engineering **4**, 261 (2002).

[3] A. Groisman, M. Enzelberger, and S. R. Quake, Microfluidic Memory and Control Devices, vol. 300: American Association for the Advancement of Science, 2003, pp. 955.

[4] J. P. Urbanski, W. Thies, C. Rhodes, S. Amarasinghe, and T. Thorsen, Lab on a Chip **6**, 96 (2006).

[5] M. Prakash and N. Gershenfeld, Science **315**, 832 (2007).

[6] N. Gleichmann, D. Malsch, M. Kielpinski, W. Rossak, G. Mayer, and T. Henkel, Chemical Engineering Journal **135**, 210 (2008).

[7] I. Inoue, Y. Wakamoto, H. Moriguchi, K. Okano, and K. Yasuda, Lab on a Chip **1**, 50 (2001).

[8] C. L. Hansen, E. Skordalakes, J. M. Berger, and S. R. Quake, Proceedings of the National Academy of Sciences of the United States of America **99**, 16531 (2002).

[9] C. D. Chin, V. Linder, and S. K. Sia, Lab on a Chip **7**, 41 (2007).

[10] D. Psaltis, S. R. Quake, and C. Yang, Nature **442**, 381 (2006).

[11] R. L. Ewing and H. S. Abdel-Aty-Zohdy, Proceedings of the 2003 International Conference on Microelectronics Systems Education, (2003).

[12] H. M. Shapiro, Practical flow cytometry, 4th ed., (Wiley-Liss New York, Hoboken, NY, 2003).

[13] A. L. Givan, Flow Cytometry: First Principles, 2nd ed., (Wiley-Liss, Inc., New York, 2001).

[14] W. G. Telford, in "Small Lasers in Flow Cytometry," in Methods in Molecular Biology: Flow Cytometry Protocols, T. S. H. a. R. G. Hawley, 2nd. Totowa, NJ: Humana Press Inc, 2004.

[15] D. Sobek, A. M. Young, M. L. Gray, and S. D. Senturia, Proceedings of Micro Electro Mechanical Systems, 1993, pp. 219.

[16] E. Altendorf, D. Zebert, M. Holl, and P. A. Yager, International Conference on Solid State Sensors and Actuators, Chicago, 1997, pp. 531.

[17] Y. Xia and G. M. Whitesides, Angewandte Chemie International Edition **37**, 550 (1998).

[18] M. A. Unger, H.-P. Chou, T. Thorsen, A. Scherer, and S. R. Quake, Science **288**, 113 (2000).

[19] M. L. Chabinyc, D. T. Chiu, J. C. McDonald, A. D. Stroock, J. F. Christian, A. M. Karger, and G. M. Whitesides, Anal. Chem. **73**, 4491 (2001).

[20] K. Haubert, T. Drier, and D. Beebe, Lab on a Chip **6**, 1548 (2006).

[21] G.-B. Lee, B.-H. Hwei, and G.-R. Huang, Journal of Micromechanics and Microengineering **11**, 654 (2001).

[22] N. Pamme, R. Koyama, and A. Manz, Lab on a Chip **3**, 187 (2003).

[23] C. H. Lin and G. B. Lee, Journal of Micromechanics and Microengineering **13**, 447 (2003).

[24] P. K. Wong, Y.-K. Lee, and C.-M. Ho, Journal of Fluid Mechanics **497**, 55 (2003).

[25] J. B. Knight, A. Vishwanath, J. P. Brody, and R. H. Austin, Physical Review Letters **80**, 3863 (1998).

[26] G.-B. Lee, C.-I. Hung, B.-J. Ke, G.-R. Huang, B.-H. Hwei, and H.-F. Lai, Transactions of the ASME **123**, 672 (2001).

[27] G.-B. Lee, C.-C. Chang, S.-B. Huang, and R.-J. Yang, Journal of Micromechanics and Microengineering **16**, 1024 (2006).

[28] D. Huh, Y.-C. Tung, H.-H. Wei, J. B. Grotherg, S. J. Skerlos, K. Kurabayashi, and S. Takayama, Biomedical Microdevices **4**, 141 (2002).

[29] T. Stiles, R. Fallon, T. Vestad, J. Oakey, D. W. M. Marr, J. Squier, and R. Jimenez, Microfluid Nanofluid **1**, 280 (2005).

[30] D. P. Schrum, C. T. Culbertson, S. C. Jacobson, and J. M. Ramsey, Anal. Chem **71**, 4173 (1999).

[31] H.-P. Chou, C. Spence, A. Scherer, and S. Quake, Proc. Natl. Acad. Sci USA **96**, 11 (1999).

[32] L.-M. Fu, R.-J. Yang, and G.-B. Lee, Anal. Chem **75**, 1905 (2003).

[33] G.-B. Lee, L.-M. Fu, R.-J. Yang, Y.-J. Pan, and C.-H. Lin, The 12th International Conference on Solid State Sensors, Actuators and Microsystems, Boston, 2003, pp. 1895.

[34] H. Morgan, D. Holmes, and N. G. Green, IEE Proc.-Nanobiotechnol **150**, 76 (2003).

[35] C.-H. Lin, G.-B. Lee, L.-M. Fu, and B.-H. Hwey, Journal of microelectromechanical systems **13**, 923 (2004).

[36] A. Wolff, I. R. Perch-Nielsen, U. D. Larsen, P. Friis, G. Goranovic, C. R. Poulsen, J. P. Kutter, and P. Telleman, Lab on a Chip **3**, 22 (2003).

[37] H. Klank, G. Goranovic, J. P. Kutter, H. Gjelstrup, J. Michelsen, and C. H. Westergaard, Journal of Micromechanics and Microengineering **12**, 862 (2002).

[38] C.-C. Chang, Z.-X. Huang, and R.-J. Yang, Journal of Micromechanics and Microengineering **17**, (2007).

[39] C. Simonnet and A. Groisman, Applied Physics Letters **87**, 114104 (2005).

[40] R. Yang, D. L. Feeback, and W. Wanga, Sensors and Actuators **A 118**, 259 (2005).

[41] N. Sundararajan, M. S. Pio, L. P. Lee, and A. A. Berlin, Journal of Microelectromechanical systems **13**, 559 (2004).

[42] X. Mao, J. R. Waldeisen, and T. J. Huang, Lab On a Chip **7**, 1260 (2007).

[43] J. Kruger, K. Singh, A. ONeill, C. Jackson, A. Morrison, and P. OBrien, Journal of Micromechanics and Microengineering **12**, 486 (2002).

[44] S. Kostner and M. J. Vellekoop, Sensors & Actuators: B. Chemical (2007).

[45] Y.-C. Tung, M. Zhang, C.-T. Lin, K. Kurabayashi, and S. J. Skerlos, Sensors and Actuators B: Chemical **98**, 356 (2004).

[46] C. L. Bliss, J. N. McMullin, and C. J. Backhouse, Lab on a Chip **7**, 1280 (2007).

[47] K. B. Mogensen, N. J. Petersen, J. Hübner, and J. P. Kutter, Electrophoresis **22**, 3930 (2001).

[48] J. N. McMullin, H. Qiao, S. Goel, C. L. Ren, and D. Li, Journal of Micromechanics and Microengineering **15**, 1810 (2005).

[49] D. Spicer, J. N. McMullin, and H. Rourke, Journal of Micromechanics and Microengineering **16**, 1674 (2006).

[50] S. H. Huang and F. G. Tseng, Journal of Micromechanics and Microengineering **15**, 2235 (2005).

[51] V. Lien, H. Lin, J. Chuang, M. J. Sailor, and Y. H. Lo, Engineering in Medicine and Biology Society, 2004. EMBC 2004. Conference Proceedings. 26th Annual International Conference of the **1** (2004).

[52] V. Lien, Y. Berdichevsky, Y. H. Lo, J. Khandurina, and A. Guttman, Lasers and Electro-Optics, 2003. CLEO03. Conference on, **4** (2003).

[53] D. B. Wolfe, R. S. Conroy, P. Garstecki, B. T. Mayers, M. A. Fischbach, K. E. Paul, M. Prentiss, and G. M. Whitesides, Proceedings of the National Academy of Sciences **101**, 12434 (2004).

[54] S. K. Y. Tang, C. A. Stan, and G. M. Whitesides, Lab on a Chip **8**, 395 (2008).

[55] S. Camou, H. Fujita, and T. Fujii, Lab on a Chip **3**, 40 (2003).

[56] K. W. Ro, K. Lim, B. C. Shim, and J. H. Hahn, Anal. Chem **77**, 5160 (2005).

[57] Z. Wang, J. El-Ali, M. Engelund, T. Gotsæd, I. R. Perch-Nielsen, K. B. Mogensen, D. Snakenborg, J. P. Kutter, and A. Wolff, Lab on a Chip **4**, 372 (2004).

[58] J. Seo and L. P. Lee, Sensors & Actuators: B. Chemical **99**, 615 (2004).

[59] J. Godin, V. Lien, and Y. H. Lo, Applied Physics Letters **89**, 061106 (2006).

[60] J. Godin, V. Lien, and Y. H. Lo, Lasers & Electro-Optics Society, IEEE **605** (2006).

[61] S. I. Chang and J. B. Yoon, The 18th Annual Meeting of the IEEE Lasers and Electro-Optics Society., 2005, pp. 749.

[62] S. I. Chang and J. B. Yoon, Optics Express **12**, 6366 (2004).

[63] S. Sinzinger and J. Jahns, Microoptics. (Wiley-VCH, 2003) pp. 22.

[64] J. Seo and L. P. Lee, Transducers, Solid-State Sensors, Actuators and Microsystems, 12th International Conference on **2** (2003).

[65] H. Jerwei, W. Chun-Jen, L. Hui-Hsiung, Hung-Ling Yin, J. Y. C. Hu, Hsiao-Yu Chou, Cheng-Fung Lai, and Weileun Fang, Optical MEMS, 2003 IEEE/LEOS International Conference on, 2003, pp. 65.

[66] H. B. Steen, Cytometry **13**, 822 (1992).

[67] J. C. Galas, J. Torres, M. Belotti, Q. Kou, and Y. Chen, Applied Physics Letters **86**, 264101 (2005).

[68] G. Goddard, J. C. Martin, M. Naivar, P. M. Goodwin, S. W. Graves, R. Habbersett, J. P. Nolan, and J. H. Jett, Cytometry Part A **69**, 842 (2006).

[69] O. Hofmann, X. Wang, A. Cornwell, S. Beecher, A. Raja, D. D. C. Bradley, A. J. deMello, and J. C. deMello, Lab on a Chip **6**, 981 (2006).

[70] D. B. Wolfe, D. V. Vezenov, B. T. Mayers, G. M. Whitesides, R. S. Conroy, and M. G. Prentiss, Applied Physics Letters **87**, 181105 (2005).

[71] S. Balslev, B. Bilenberg, O. Geschke, A. M. Jorgensen, A. Kristensen, J. P. Kutter, K. B. Mogensen, and D. Snakenborg, Micro Electro Mechanical Systems, 2004. 17th IEEE International Conference on. (MEMS) **89** (2004).

[72] Z. Li and D. Psaltis, Microfluidics and Nanofluidics **4**, 145 (2008).

[73] V. Lien, K. Zhao, Y. Berdichevsky, and Y. H. Lo, Selected Topics in Quantum Electronics, IEEE Journal of **11**, 827 (2005).

[74] J. A. Shizuru, R. S. Negrin, and I. L. Weissman, Annual Review of Medicine **56**, 509 (2005).

[75] H. J. Gross, B. Verwer, D. Houck, R. A. Hoffman, and D. Recktenwald, Proc Natl Acad Sci USA **92**, 537 (1995).

[76] W. R. Rodriguez, N. Christodoulides, P. N. Floriano, S. Graham, S. Mohanty, M. Dixon, M. Hsiang, T. Peter, S. Zavahir, I. Thior, D. Romanovicz, B. Bernard,

A. P. Goodey, B. D. Walker, and J. T. McDevitt, PLoS Medicine **2**, e182 (2005).

[77] J. L. Zabzdyr and S. J. Lillard, Trends in Analytical Chemistry **20**, 467 (2001).

[78] A. Y. Fu, C. Spence, A. Scherer, F. H. Arnold, and S. R. Quake, Nature Biotechnology **17**, 1109 (1999).

[79] N. T. Nguyen and S. T. Wereley, Fundamentals and Applications of Microfluidics. (Artech House, 2002).

[80] L. M. Fu, R. J. Yang, C. H. Lin, Y. J. Pan, and G. B. Lee, Analytica Chimica Acta **507**, 163 (2004).

[81] P. S. D. a. P. Schwille, Anal. Chem. **75**, 5767 (2003).

[82] A. Y.-C. Fu, Microfabricated Fluorescence-Activated Cell Sorters (FACS) for Screening Bacterial Cells, vol. Ph. D. Pasadena: California Institute of Technology, pp. 115.

[83] J. Berthier and P. Silberzan, Microfluidics for Biotechnology. (Artech House, Inc, Norwood, 2006), pp. 345.

[84] S. Fiedler, S. G. Shirley, T. Schnelle, and G. Fuhr, Anal. Chem **70**, 1909–915 (1998).

[85] J. Voldman, M. L. Gray, M. Toner, and M. A. Schmidt, Anal Chem **74**, 3984 (2002).

[86] E. B. Cummings and A. K. Singh, Anal. Chem **75**, 4724 (2003).

[87] M. Frenea, S. P. Faure, B. L. Pioufle, P. Coquet, and H. Fujita, Mat. Sci. Eng. **23**, 597 (2003).

[88] T. Schnelle, T. Muller, C. Reichle, and G. Fuhr, Applied Physics B. **70**, 267 (2000).

[89] B. H. Lapizco-Encinas, B. A. Simmons, E. B. Cummings, and Y. Fintschenko, Electrophoresis **25**, 1695 (2004).

[90] I. Barbulovic-Nad, X. Xuan, J. S. H. Lee, and D. Li, Lab on a Chip **6**, 274 (2006).

[91] K. H. Kang, Y. Kang, X. Xuan, and D. Li, Electrophoresis **27**, 694 (2006).

[92] D. Holmes, M. E. Sandison, N. G. Green, and H. Morgan, Nanobiotechnology, IEE Proceedings-**152**, 129 (2005).

[93] K. Ahn, C. Kerbage, T. P. Hunt, R. M. Westervelt, D. R. Link, and D. A. Weitz, Applied Physics Letters **88**, 024104 (2006).

[94] I. Doh and Y.-H. Cho, Sensors and Actuators A **121**, 59 (2005).

[95] T. Braschler, N. Demierre, E. Nascimento, T. Silva, A. G. Oliva, and P. Renaud, Lab on a Chip **8**, 280 (2007).

[96] X. Hu, P. H. Bessette, J. Qian, C. D. Meinhart, P. S. Daugherty, and H. T. Soh, PNAS **102**, 15757 (2005).

[97] P. H. Bessette, X. Hu, H. T. Soh, and P. S. Daugherty, Anal. Chem **79**, 2174 (2007).

[98] A. Ito, M. Shinkai, H. Honda, and T. Kobayashi, Journal of Bioscience and Bioengineering **100**, 1 (2005).

[99] C. Billotey, C. Wilhelm, M. Devaud, J. C. Bacri, J. Bittoun, and F. Gazeau, Magnetic Resonance in Medicine **49**, 646 (2003).

[100] Z. H. Fan, S. Mangru, R. Granzow, P. Heaney, W. Ho, Q. Dong, and R. Kumar, Anal. Chem **71**, 4851 (1999).

[101] G. Jiang and D. J. Harrison, The Analyst **125**, 2176 (2000).

[102] N. Pamme and C. Wilhelm, Lab on a Chip **6**, 974 (2006).

[103] N. Pamme and A. Manz, Anal Chem **76**, 7250 (2004).

[104] N. Xia, T. P. Hunt, B. T. Mayers, E. Alsberg, G. M. Whitesides, R. M. Westervelt, and D. E. Ingber, Biomedical Microdevices **8**, 299 (2006).

[105] H. Bang, C. Chung, J. K. Kim, S. H. Kim, S. Chung, J. Park, W. G. Lee, H. Yun, J. Lee, K. Cho, D.-C. Han, and J. K. Chang, Microsystem Technology **12**, 746 (2006).

[106] A. Y. Fu, H.-P. Chou, C. Spence, F. H. Arnold, and S. R. Quake, Analytical Chemistry **74**, 2451 (2002).

[107] M. A. Unger, H.-P. Chou, Todd Thorsen, A. Scherer, and S. R. Quake, Science **288**, 113 (2000).

[108] V. Studer, R. Jameson, E. Pellereau, A. P. epin, and Y. Chen, Microelectronic Engineering **73/74**, 852 (2004).

[109] G. Blankenstein and U. Darling Larsen, Biosensors and Bioelectronics **13**, 427 (1998).

[110] J. Krüger, K. Singh, A. ONeill, C. Jackson, A. Morrison, and P. OBrien, J. Micromech. Microeng. **12**, 486 (2002).

[111] C. H. Chen, S. H. Cho, A. Erten, and Y.-H. Lo, "High-speed hydrodynamic manipulation of single cells on a piezoelectric actuator integrated microfluidic device," 2008.